Deep Sea Research Part I: Oceanographic Research Papers
February 2024, Volume 204 Pages 104221 (14p.)
https://doi.org/10.1016/j.dsr.2023.104221
https://archimer.ifremer.fr/doc/00869/98108/

Comparative analysis of day and night micronekton abundance estimates in west pacific between acoustic and trawl surveys

Barbin Laure [1, 2, *], Lebourges-Dhaussy Anne [2], Allain Valerie [3], Receveur Aurore [4], Lehodey Patrick [3, 5], Habasque Jeremie [2], Vourey Elodie [3], Portal Annie [3], Roudaut Gildas [2], Menkes Christophe [1]

[1] ENTROPIE, UMR 9220, IRD, Univ. de La Réunion, CNRS, 101 Promenade Roger Laroque, 98800, Noumea, New Caledonia
[2] IRD, University of Western Brittany, CNRS, Ifremer, LEMAR, Campus Ifremer, BP70, 29280, Plouzané, France
[3] OFP/FAME Division, Pacific Community, 95 Promenade Roger Laroque, BP D5, 98848, Noumea, New Caledonia
[4] CESAB - FRB, 5 Rue de L'École de Médecine, 34000, Montpellier, France
[5] Mercator Ocean International, Toulouse, France

* Corresponding author : Laure Barbin, email address : laure.barbin@ird.fr

Abstract :

Micronekton organisms are a central component of the trophic organization in the pelagic ecosystem, being prey to top predators and participating in the export of carbon from the surface to the deep layers. Despite their importance, the abundancedeep sea estimates and species distribution of micronekton remain largely uncertain. This study aimed to compare and assess two sampling methods classically used for the estimation of micronekton abundance in mesopelagic acoustic scattering layers: scientific echosounder and trawl sampling. Measurements of 38 and 70 kHz hull-mounted echosounders were examined with biological trawl samples from 8 surveys in the South-West tropical Pacific. A model of acoustic observation was built from the trawl sampling species composition and forward scattering models. Predicted and observed acoustic responses are compared to assess the variability and the difference between the acoustic and trawl sampling methods in various scattering layers, for day and night periods. The difference between methods decreased with depth and with increasing abundance of fish with swimbladders caught in trawls. Notably, this difference was found to be minimal in the nocturnal deep scattering layer (mesopelagic zone, depth>200 m). This study emphasizes potential lower estimates of organisms' abundance by trawling and a bias towards mesopelagic fish. Understanding the differences between methods and their variability within different scattering layers is essential for studying micronekton and improving the precision of biomass estimates.

Highlights

► Acoustic-trawl surveys in scattering layers of West tropical Pacific. ► Forward scattering models applied to micronekton trawl sampling with a high species diversity. ► The difference in micronekton density estimates between acoustic and trawl methods varies across scattering layers. ► The disparities between methods decrease in night mesopelagic layers and trawls with high swimbladdered fish density.

Keywords : West tropical Pacific, Scattering models, Mesopelagic fish, Target strength, Scattering layers

Introduction

Micronekton, ubiquitous to all oceans and distributed in mesopelagic acoustic scattering layers plays a pivotal role in the trophic organisation of the pelagic ecosystem. It feeds on zooplankton and serves as prey for mid-level and top predators, including tuna (Bertrand et al., 2002; Young et al., 2015).

Micronekton are defined by a size range from 2 to 20 cm and encompasses a large variety of species that can be classified into large taxonomic categories: fishes including mesopelagic fish, crustaceans, gelatinous organisms, and molluscs (including squids) (Blackburn, 1968; Brodeur et al., 2004; Escobar-Flores et al., 2019). A significant portion of species of micronekton, which has been estimated to be 78% in the Coral Sea (Receveur et al., 2020a), undertakes a diel vertical migration (DVM). They migrate from the deeper layers (200-1000m), where they reside during the daytime, to the surface layers (epipelagic: 0-200m or upper-mesopelagic: 200-500m) at night (Pearre, 2003; Brierley, 2014; Czudaj et al., 2021). This migration pattern contributes to the biogeochemical fluxes between the surface and the mesopelagic domain (Davison et al., 2013; Ariza et al., 2015; Anderson et al., 2019). The frequent distribution of micronekton in dense scattering layers in the upper 1000m of the water column varying with time and space (Burgos and Horne, 2008; Benoit-Bird and Lawson, 2016) poses challenges for their study.

Micronekton, with their significant contribution to the overall biomass of the oceans, present a challenge for accurate biomass estimates due to their high species diversity. Estimates often focus more specifically on a taxonomic group, such as mesopelagic fish or krill. When considering mesopelagic fish biomass, trawl sampling provides the lowest estimate around 1 billion tons (Gjøsæter and Kawaguchi, 1980). Acoustic studies show median estimates between 3.8 and 15 billion tons (Irigoien et al., 2014). Proud et al. (2019) further refines this range to 3.8 to 8.3 billion tons, accounting for factors like the proportion of mesopelagic fish without gas-filled inclusion and the contribution of other micronekton organisms. Additionally, ecosystem-based trophic models bridge the gap between acoustic studies and historical trawl sampling estimates, predicting a mesopelagic fish biomass of 2.4 billion tons (Anderson et al., 2019), which is 26 to 130% higher than Hill Cruz et al. (2023) estimates.

The significant variability in biomass estimates of mesopelagic fish and the difficulty to include all taxa of micronekton can be attributed to biases inherent to each of the two methods. The acoustic provides a proxy of the density of organisms throughout the water column and the single narrowband 38kHz is commonly employed to investigate the biomass of mid-trophic organisms, particularly mesopelagic fishes, within the depth range from the surface down to 1000 meters (Kloser et al., 2009; De Robertis et al., 2017b; Receveur et al., 2020a). Interpreting the backscattered volume using this single frequency is quite challenging in ecosystems characterized by a wide diversity of taxa and mixed scattering layers. Dominant scatterers, which include organisms with gas-filled inclusions, tend to mask the response of the weaker scatterers, such as crustaceans and fish lacking gas-bladder (Mair et al., 2005; Davison et al., 2015; Dornan et al., 2019, 2022). Furthermore, the target strength (TS), which represents the individual acoustic response of organisms, varies depending on their size and orientation within a species (McGehee et al., 1998; Scoulding et al., 2017). The insonified volume increases with the distance to the echosounder, thereby potentially increasing the number and diversity of the scattering organisms' taxa detected with depth in the mean backscattered response, further complicating its interpretation.

Regarding the pelagic trawl sampling method, it is an essential tool to collect biological samples from specific depth layers in order to assess the taxonomic diversity of organisms (Receveur et al., 2020b). However, relying solely on this method for estimating the abundance of mesopelagic organisms introduces biases, primarily due to avoidance behaviour exhibited by nektonic organisms (Kaartvedt et al., 2012), variable catchability among species (Arreguín-Sánchez, 1996; De Robertis et al., 2017; Underwood et al., 2020) and selectivity associated with trawl mesh size (Heino et al., 2011; Grimaldo et al., 2022).

Therefore, examining the acoustic backscatter in conjunction with *in situ* biological sampling is essential for accurate estimation of micronekton density and diversity (McClatchie et al., 2000). Understanding the morphological characteristics of species within scattering layers (Kloser et al., 2009; Dornan et al., 2022) enables the investigation of their contributions to the acoustic backscattered signal (Scoulding et al., 2017). Combined acoustic-trawls studies have demonstrated successful estimation of mesopelagic fish biomass in ecosystems with low species diversity (De Robertis et al., 2017b; Scoulding et al., 2017). However, the uncertainty in biomass estimates tends to increase with the biodiversity in ecosystems. There is uncertainty regarding whether trawls tend to underestimate the abundance of organisms and fail to provide a homogeneous sampling of all species (Mair et al., 2005; Kloser et al., 2009; Blanluet et al., 2019). Although imperfect, trawls remain essential for understanding the composition of scatterers in ecosystems, and in particular the proportion of weak and strong scatterers (Dornan et al., 2022). Due to the paucity of sampling and inherent biases associated with trawl and acoustic methods, precise estimations of the abundance and species distribution of micronekton organisms remain highly uncertain when accounting for all taxa (St. John et al., 2016; Hidalgo and Browman, 2019; Fjeld et al., 2023). This is particularly the case for mesopelagic communities in the tropical Pacific (Klevjer et al., 2020; Ariza et al., 2022), further amplifying the uncertainty regarding micronekton abundance.

The present study aims at interpreting acoustics at 38 and 70 kHz relative to trawl sampling in the tropical southwest Pacific. Comparison of acoustics and biological sampling is achieved through forward method, which converts trawl species composition and abundances into volume backscatter. This method uses theoretical scattering models and biological samplings from midwater trawls collected during 8 surveys providing species densities, sizes and distributions (e.g. Blanluet et al., 2019). This approach predicts the theoretical mean volume backscattered signal in the scattering layers, considering all captured taxa, and compares it to the mean volume backscatter from the hull-mounted echosounder. The disparities between the two acoustic densities in relation to the time-period, sampling depth and trawl composition were explored within various scattering layers. This study highlights the complexity of estimating micronekton densities in environments with high biodiversity, and the need to resolve the main causes of discrepancies between these two complementary observation methods to better estimate biomass and clarify the uncertainty on this estimate.

1. Materials and methods

Data used in this paper were collected during eight research cruises spanning 2011-2021 (Nectalis 1-5, Wallalis, KANARECUP and WARMALIS-1, referred to as NEC1-5, WAL, KANA and WARM) in the western tropical Pacific region (Figure 1, Table 1). The cruises covering the area between 157°E-176°W and 4°N-26°S were conducted on board R/V Alis (French oceanographic fleet) with the objective of understanding the mechanisms structuring the pelagic ecosystem that supports tuna fisheries in the region. All surveys included hull-mounted narrowband data and micronekton trawl sampling, where the acoustic recordings and trawls were conducted simultaneously.

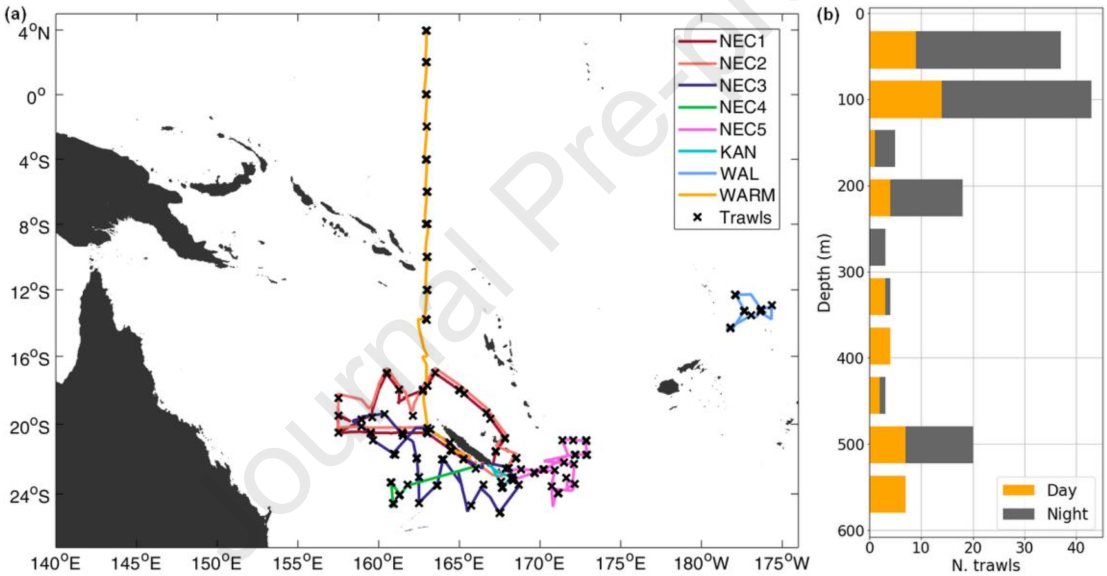

Figure 1. Map of the south-western Pacific Ocean, showing (a) cruise tracks with the R/V Alis. NEC1 and NEC2 tracks partially overlap. The NEC2 track was therefore artificially shifted to the north for visualization purposes. Black crosses represent trawl sampling stations. Dark grey areas illustrate lands above sea surface level. (b) Number of trawls per depth colored by time of the day. Depth refers to the average towing depth during fishing.

Table 1. Details of the 8 cruises aboard R/V Alis, with the cruise name, start and end dates, locations and number of trawls used in this study. EEZ is for Economic Exclusive Zone.

Cruise name	Time Period	Location	Number of trawls
Nectalis 1 [a]	30/07/2011 – 15/08/2011	New-Caledonia EEZ	15
Nectalis 2 [b]	26/11/2011 – 14/12/2011	New-Caledonia EEZ	25
Nectalis 3 [c]	21/11/2014 – 08/12/2014	New-Caledonia EEZ	26
Nectalis 4 [d]	19/10/2015 – 25/10/2015	New-Caledonia EEZ	8
Nectalis 5 [e]	23/11/2016 – 06/12/2016	New-Caledonia EEZ	30
Wallalis [f]	01/07/2018 – 16/07/2018	Wallis-and-Futuna EEZ	11
Kanarecup [g]	19/12/2020 – 11/05/2021	New-Caledonia EEZ	7

Warmalis 1 [h]	06/09/2021 – 03/10/2021	West tropical Pacific Ocean	22

a. Allain and Menkes (2011a), b. Allain and Menkes (2011b), c. Allain and Menkes (2014), d. Allain and Menkes (2015), e. Allain and Menkes (2016), f. Allain and Menkes (2018), g. Olu and Allain (2020), h. Menkes and Allain (2021).

1.1 Acoustic data

Acoustic narrowband data at 38 and 70 kHz were recorded continuously with a calibrated (Foote et al., 1987; Demer et al., 2015) hull-mounted EK60 echosounder (SIMRAD Kongsberg Maritime AS, Horten, Norway) using two split-beam transducers. The sounder was located at 3.1m below the surface. The acquisition and calibration parameters are described in Supplementary Table S1. The water column was sampled down to 800 m and 400 m depth for 38 and 70 kHz, respectively, except for NEC1, where the range was limited at 600 m for the 38 kHz.

The raw acoustic data were pre-processed using the open source tool "Matecho" (Perrot et al., 2018) developed by the French National Research Institute for Sustainable Development (IRD), which incorporates the "Movies3D" software developed at the French Research Institute for Exploitation of the Sea (IFREMER; Trenkel et al., 2009). The pre-processing steps followed the procedures described in Receveur et al. (2020a). The volume backscattering strength was then echo-integrated between 8 and 600 m depth onto 1 m depth interval over an Elementary Distance Sampling Unit (EDSU) of 0.1 nmi, with a -100 dB threshold. The acoustic mean volume backscattering strength $\mathrm{S_v}$ (in dB re 1 m^{-1}) was calculated as $\mathrm{S_v}=10\log(\mathrm{s_v})$, with $\mathrm{s_v}$ the volume backscattering coefficient in m^{-1} (MacLennan et al., 2002). Migration periods (dusk and dawn) were excluded by considering the solar elevation angle, removing EDSU with an altitude angle between 0° and 18° (Lehodey et al., 2015).

Mean $\mathrm{S_v}$ in trawled scattering layers. At each trawl station, the average $\mathrm{S_v}$ was determined from the echosounder within the sampled layer by overlaying trawl tracks onto echo-integrated echograms (Figure 2). As the trawl was towed behind the vessel, acoustic data were not exactly simultaneously recorded during trawling. The offset time of the trawl relative to the echosounder was adjusted by using the mean vessel speed over the tow and computing the trawl wire length at the maximum towing depth. The $\mathrm{S_v}$ values were extracted along the trawl track within the towing depth layer interval indicated by the solid lines in Figure 2 and averaged (in the linear domain) to obtain the mean $\mathrm{S_{v,obs}}$ for trawl. The areas of hauling and setting (Figure 2, dashed lines) were excluded of $\mathrm{S_{v,obs}}$. Sampling depth of each trawl was estimated as the mean depth during towing and referred as $\mathrm{d_{trawl}}$.

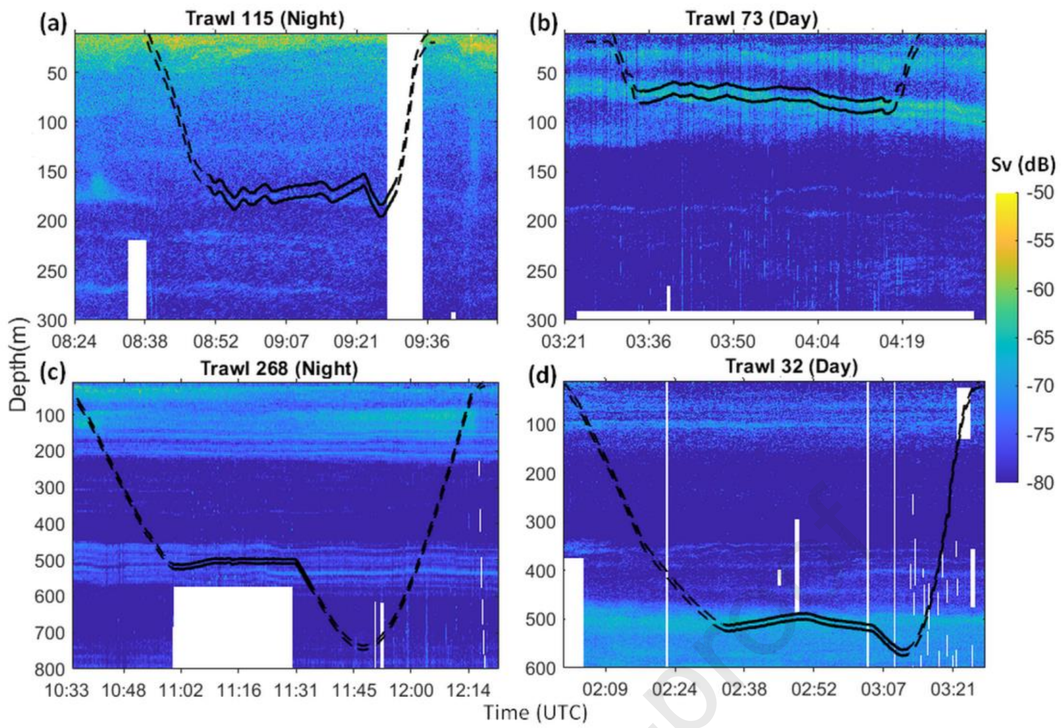

Figure 2. Examples of extraction of $S_{v,obs}$ during trawling at 38 kHz. Echogram from EK60 at 38 kHz acquired while trawling in the epipelagic layer: (a) trawl #115 (night-time, during NEC5) and (b) #73 (day-time, during NEC3) and in the mesopelagic layer: (c) trawl #268 (night, during WARM) and (d) #32 (day, during NEC2). The colorscale indicates the mean volume backscattering strength (S_v in dB re 1 m^{-1}). The trawl track is shown in black lines. The solid lines indicate the towing layer when fishing, used to calculate d_{trawl} and compute $S_{v,obs}$, while the dotted line represents the setting and hauling periods. White areas show acoustic data excluded during pre-processing.

1.2 Micronekton trawl sampling

A total of 190 small pelagic mid-water trawls were conducted during the 8 campaigns (Figure 1). The trawl had a length of 55m and a mesh size that gradually decreased from 80mm at the mouth to 10mm at the cod-end. The average vertical and horizontal opening of 10m were monitored during trawling, along with depth using four acoustic-net-monitoring systems (Scanmar AS, SS4 Depth Sensor) attached to the headline, footrope and wings of the net. Prior to each trawl, the target depth was determined based on real-time analysis of acoustic data, aiming to target the scattering layers with the highest acoustic density. Once stabilized at the selected depth, the trawl was towed horizontally for 30 minutes at an average speed of 3 knots. All trawls were conducted similarly, at the exception of the epipelagic trawls (d_{trawl}<200 m) during WARM, where oblique tows were performed between the surface and 200 m depth. On board the vessel, biological samples were sorted by broad taxon (e.g. fishes, crustaceans, cephalopods and gelatinous organisms), before being frozen at -20°C. In the laboratory at the Pacific Community (SPC), the thawed specimens were counted, weighted, and further examined to identify the species. While we aimed to identify specimens to the more precise taxon possible, gelatinous organisms, in particular, were challenging to identify accurately due to the damage caused by trawling and the difficulty of identification after thawing. Siphonophores, being colonial organisms that may be separated during trawling, were particularly challenging to count and measure. Therefore, the mean length of siphonophores was not included in the description of acoustic categories in Table 2.

To apply forward scattering models to trawl samples, the species were classified into different groups based on their acoustic properties. These groups, referred to as acoustic categories subsequently, included fish with gas-filled swimbladder (abbreviated in fish with swimbladders or SWB), fish without swimbladder, decapods and euphausiids, amphipods, squids, jellyfishes, other gelatinous organisms (abbreviated as gelatinous), elastic-shelled pteropods (abbreviated as shelled pteropods), and siphonophores bearing a pneumatophore (Table 2). Fish were divided in two categories based on the presence or absence of a gas-filled swimbladder, determined from literature and considering their species and developmental stage (see Supplementary S2). When no information was available, the taxa was assigned to the category most represented in its Family (Marohn et al., 2021). Fish without swimbladder included three types of fish: i) species that lack gas-filled inclusions throughout their entire life cycle, 2) adult fish of species that possess a swimbladder only during their juvenile stage while the swimbladder regresses at the adult stage and 3) fish bearing a lipid-invested swimbladder. As a result, depending on the developmental stage of each specimen, a species could be classified in both fish with swimbladders and fish without swimbladder.

The density of organisms (ρ_T, in individuals/1000m^3) was calculated for every acoustic category in each trawl. The volume of water sampled by the trawl ($V_{sampled}$) was estimated based on the distance covered by the trawl during fishing and the trawl opening (as in Receveur et al., 2020b). The periods of hauling and setting were not included (see Figure 2). Trawls conducted during migration periods (dusk and dawn) were excluded, accounting for approximately 10% of the total trawls.

Table 2. Description of taxonomic groups used as acoustic categories of specimens sampled with the trawl. The frequency of presence of each categories in all trawls (% trawls), mean length (in mm) and standard deviation, mean weight (in grams) and standard deviation, number of taxa in each category and the two main taxa found in each category in percentage of occurrence in the category and in the total catches were indicated. The more precise taxonomic level of identification is indicated by superscript numbers after taxon names: 1.Genus, 2.Subfamily, 3.Family, 4.Suborder.

Taxonomic group	Presence (% trawls)	Mean length (mm)	Mean wet weight (g)	Taxa richness (N. of taxa)	Two most abundant taxa (% within group, % across group)
Fish with swimbladders	98	42 (21)	189 (280)	310	*Ceratoscopelus warmingii* (33, 12) *Polyipnus* sp. [1] (8, 3)
Fish without swimbladder	98	83 (66)	81 (121)	102	Bathymyrinae [2] (11, 1) *Lobianchia gemellarii* (8, 0.5)
Decapods & Euphausiids	97	28 (10)	23 (34)	109	*Thysanopoda tricuspidata* (19, 3) *Euphausia mucronata* (16, 2)
Amphipods	80	20 (11)	3 (5)	35	*Phronima* sp. [1] (56, 2) *Phronima sedentaria* (15, 0.5)

Gelatinous	88	25 (20)	61 (77)	36	Pyrosomatidae [3] (36, 12) *Pyrosoma atlanticum* (14, 5)
Squids	91	44 (30)	66 (120)	76	*Abraliopsis* sp. [1] (22, 1) *Pterygioteuthis microlampas* (19, 1)
Jellyfishes	54	24 (20)	7 (11)	21	Bougainvilliidae [3] (20, 0.3) *Alatina* sp. [1] (11, 0.1)
Shelled pteropods	68	5 (3)	2 (2)	30	*Clio* sp. [1] (45, 0.2) *Cavolinia* sp. [1] (15, 0.1)
Siphonophores with pneumatophore	9	NA	3 (3)	3	Physonectae [4] (47, 0.2) Agalmatidae [3] (47, 0.2)

1.3 Forward scattering models

In order to compare echosounder backscatter and trawl density (ρ_T), target strength (TS, in dB re 1 m²) scattering models were applied to the trawl's biological samples to calculate the theoretical response of the specimen. A mean backscattering volume $S_{v\ mod}(f)$ was determined for each trawl by making an incoherent weighted summation of the contributions from all acoustic categories in the linear domain (Foote, 1983; Stanton et al., 2012), where the organisms' density served as the weighting factors (Figure 3). All categories are associated to a scattering model with taxa-specific input parameters, applied on the frequency interval 1-200kHz.

Gas-bearing organisms. The acoustic categories of *fish with swimbladders* and *siphonophore with pneumatophore* are organisms bearing a gas-filled inclusion surrounded by a weakly scattering fluid-like body. For fish with a swimbladder, the volume of the fish body (V_f) was approximated as a prolate spheroid with the measured fish length (L_f) as the major axis and L_f/α_f as the minor axis. The fish aspect ratio (α_f) is equal to 5. The swimbladder size was calculated with the equivalent spherical radius $a_{esr} = (\frac{3p_{swb}V_f}{4\pi})^{1/3}$, where p_{swb} was the percentage of V_f used for the swimbladder (Proud et al., 2019). The value p_{swb}=2.5% as reported in Blanluet et al. (2019) was used. The swimbladder backscatter was described using a hybrid scattering model. For lower frequencies ($ka_{esr} \leq 0.2$, , where k was the wave number in m^{-1}), backscatter was computed using a resonance-scattering model from Scoulding et al. (2015, 2022). This model takes into account the increased backscattering response resulting from the elongation of the swimbladder into a prolate spheroid as defined in Ye (1997) along with a directivity term relative to the incident sound wave and the fish's tilt angle (θ in radians). At broadside incidence ($\theta = \pi/2$), the directivity term was equal to one. The prolate spheroid elongation was defined by a length-to-width aspect ratio (b/a) of 1.5, with *a* and *b* the semi-major and semi-minor axis, respectively. For higher frequencies ($ka_{esr} > 0.2$), the geometrical scattering effect of the swimbladder was modelled using the exact modal series solution for a fluid sphere of equivalent radius a_{esr} defined in Anderson (1950). The transition frequency between the models was chosen at the beginning of the elbow above the resonance frequency (approximately at $ka_{esr} = 0.2$).

In the case of siphonophores, the mean equivalent radius a_{esr} of pneumatophore (filled with carbon monoxide gas: g = 0.0012 and h = 0.22 from Benfield et al. (2003) and Lavery et al. (2007)) was fixed at 0.5 mm, based on Benfield et al. (2003), Kloser et al. (2016) and Proud et al. (2019). The scattering from the fish body and the nectophores (fluid-like parts of the siphonophore) were considered to be neglectable (Scoulding et al., 2015). The specific shape and physical model parameters for both categories are summarized in Table 3.

Elastic shell organisms. The *shelled pteropods* acoustic category was similar to a fluid-like sphere surrounded by a solid shell. It was modelled with a simple high-pass dense fluid model based on Lavery et al. (2007), with a reflection coefficient R=0.5 (Blanluet et al., 2019). The equivalent spherical radius a_{esr} (in m) was estimated as half the length of the measured diameter.

Fluid-like organisms. All the remaining acoustics categories, including *amphipods*, *euphausiids and decapods*, *gelatinous*, *jellyfish*, *squid* and *fish without swimbladder* were modelled using a model based on the Distorted-Wave Born Approximation (DWBA) scattering model averaged over a normal distribution of orientation angles (Stanton et al., 1998; Stanton and Chu, 2000). The fluid-like organisms were simplified as uniformly-bent and tapered cylinders, except for jellyfish approximated as two prolate spheroidal surfaces (Warren and Smith, 2007) and integrated over 300 integration points along the body axis of total length (L). The length L was defined as the total length for *amphipods*, *euphausiids and decapods* (equivalent to Standard Length 1 in Mauchline, 1981) and *gelatinous*, the mantle length for *squid*, the standard length for *fish without swimbladder* and the bell diameter for *jellyfish*. The cylindrical cross-section radius a (in m) of the organisms was estimated with the ratio L/a summarized in Table 4. The parameters and shape of the scattering model for each category is shown Table 4. Most of the parameters are extracted from Lawson et al. (2004).

Table 3. Swimbladder and pneumatophore hybrid scattering model parameters.

Parameter	Symbol	Value for swimbladder	Value for pneumatophore	Unit
Heat ratio of gas inclusion	γ_{swb}	1.4 [a]	1.4 [a]	-
Organisms' tissue density	ρ_f	1050 [b]	1030 [c]	kg m^{-3}
Density of air	ρ_a	1.3 [b]	1.3 [b]	kg m^{-3}
Water density	ρ_w	Varying with depth [d]	Varying with depth [d]	kg m^{-3}
Sound speed	c_w	Varying with depth [e]	Varying with depth [e]	m s^{-1}
Thermal conductivity of air	k_a	5.5×10^{-3} [b]	5.5×10^{-3} [b]	cal m^{-1} s^{-1} °C^{-1}
Length/width ratio	b/a	1.5 [f]	2.35 [f]	-
Shear modulus	μ_r	5.10^5 [g]	5.10^5 [h]	N m^{-2}
Dynamic viscosity	ξ	1 [g]	4/3 [i]	kg m^{-1} s^{-1}
Surface tension	s	200 [b,g]	0.074 [i]	N m^{-1}
Heat capacity of air	c_{pa}	240 [b]	240 [b]	cal kg^{-1} °C^{-1}
Sound speed contrast	h	0.22 [j]	0.22 [c]	-

Density contrast	g	0.0012 [j]	0.0012 [c]	-
Percentage of volume of fish occupied by the swimbladder	p_{swb}	2.5 [f]	NA	%
Tilt angle	θ	0 [g]	25 [k]	°

a. Kloser et al., 2002,
b. Love, 1978,
c. Lavery et al., 2007,
d. Estimated with the closest CTD profiles
e. Calculated with the equation from Mackenzie, 1981,
f. Blanluet et al., 2019,
g. Scoulding et al., 2015,
h. Empirically chosen identical as swimbladder because we had no value available,
i. Proud et al., 2017,
j. Jech et al., 2015,
k. Empirically chosen for the pneumatophore.

Table 4. Weak scatterers models parameters for each acoustic category. Radius of curvature ρ_c/L were chosen empirically, where $\rho_c/L \rightarrow \infty$ defines a straight cylinder shape. N defines the Normal distribution.

Organism (Scattering model)	Length-to-cylindrical radius (L/a)	Orientation (Mean, STD)	Density contrast (g)	Sound speed contrast (h)	Radius of curvature (ρ_c/L)
Fishes without Swimbladder (DWBA *uniformly-bent cylinder)*	8 [a]	N(0,30) [a]	1.010 [a]	1.025 [a]	10
Amphipods (DWBA *uniformly-bent cylinder)*	3 [c]	N(0,30) [c]	1.058 [b]	1.058 [b]	6
Euphausiids, Decapods<25mm (DWBA *uniformly-bent cylinder)*	10.5 [b]	N(20,20) [b]	1.016 [b]	1.019 [b]	3
Euphausiids, Decapods>25mm (DWBA *uniformly-bent cylinder)*	10.5 [b]	N(20,20) [b]	$5.485 \times L*10^{-4}$ +1.002 [b]	$5.942 \times L*10^{-4}$ +1.004 [b]	3
Gelatinous (DWBA *uniformly-bent cylinder)*	4 [c]	N(0,30) [c]	1.003 [b]	1.003 [b]	10
Shelled pteropods (*High-pass fluid sphere)*	NA	NA	R=0.5=(gh-1)/(gh+1) [a,b]	NA	NA
Squids (DWBA *uniformly-bent cylinder)*	5 [d]	N(0,20) [d]	1.029 [d]	1.041 [d]	10
Jellyfishes (*DWBA two prolate spheroidal surfaces*)	NA	NA	1.02 [a]	1.02 [a]	NA

a. Blanluet et al., 2019,
b. Lawson et al., 2004,
c. Lavery et al., 2007,
d. Jones et al., 2009.

1.3.1 Prediction of modelled backscattering strength with forward approach

The modelled volume backscattering strength $S_{v,mod}$ was estimated for each trawl as:

$$S_{v,mod}(f) = 10log_{10}\left(\sum_{i=1}^{N_{taxa}} \rho_{T,i}\,\sigma_{bs,i}\right) \quad (1)$$

with N_{taxa} the number of taxa groups, $\rho_{T,i}$ the density in individual (N ind./$V_{sampled}$ in m^{-3}) and $\sigma_{bs,i}$ the backscattering cross-section of each taxa group i, defined as:

$$\sigma_{bs,i} = \sum_{j=1}^{n_{length\ class}} D_j^i\,{\sigma_{bs}}_j^i \quad (2)$$

For each taxa group i, ${\sigma_{bs}}_j^i$ was the modelled backscatter cross-section (in m²) of length class j. D_j^i was the proportion of individuals of length class j in the taxa group i. $S_{v,mod}(f)$ was the total theoretical backscattering response over frequency *f* and was determined for each trawl.

1.3.2 Uncertainty analysis

Model parameters for the scattering models were derived from literature. However, the variability in parameters across a wide range of taxa introduced a source of uncertainty. To assess the reliability of model predictions, 1000 simulations for each size were performed, randomly selecting input values from uniform distributions derived from maxima in literature when available or centred around the reference value (Supplementary Table S3). Uniform distributions were selected to cover the entire spectrum of variability in model parameters and their influence on the simulated backscatter (Proud et al., 2019). The uncertainty around scattering predictions was defined as the standard deviation of the simulation results over the total modelled backscatter. For the fluid-like models (DWBA), the parameters of density and sound speed contrast g and h and the aspect ratio L/a were evaluated. As for the resonant-scattering model, the parameters considered were α_f, p_{swb}, b/a and θ. The impact of the other parameters of the resonant model were considered neglectable compared to those involved in the definition of the size and shape of the gas-filled inclusion. The length of organisms was not included in the uncertainty analysis as it was measured on all organisms from net samples. The incertitude on the orientation, relative to the direction of incidence, was simulated with a normal distribution of angle in the DWBA model.

1.4 Comparison of *in situ* and modelled acoustics

This study gathered campaigns conducted over a 10 year-period with minimal variations in the sampling protocols. Notably, trawling depth was chosen depending on the scattering layers detected by the echosounder to study all types of scattering layers in most sea-experiments. Yet the most recent survey WARMALIS-1 applied a different sampling strategy where trawling was performed systematically from the surface down to 200m (oblique tow) and at 500m (horizontal tow) for each station. Whenever the quality of echosounder data was not sufficient to calculate $S_{v,obs}$ (mainly due to bad weather and a strong swell creating empty pings) the corresponding trawl was excluded from the dataset. The final dataset contained 75% of the original trawls (n=144) at 38kHz and 59% (n=112) at 70kHz.

The difference of volume backscattering strength $\Delta S_{v,f}$ between $S_{v,mod}(f)$ and $S_{v,obs}(f)$ was calculated as:

$$\Delta S_{v,f} = S_{v,obs}(f) - S_{v,mod}(f) \tag{3}$$

with $\Delta S_{v,f}$ calculated at f=38 kHz and f=70 kHz, allowing us to measure the difference between the two acoustic densities: observed and modelled from trawl. To explore the link between $\Delta S_{v,38}$ and $\Delta S_{v,70}$, a linear regression (lm) was fit to the data using R statistical software (R Core Team, 2023).

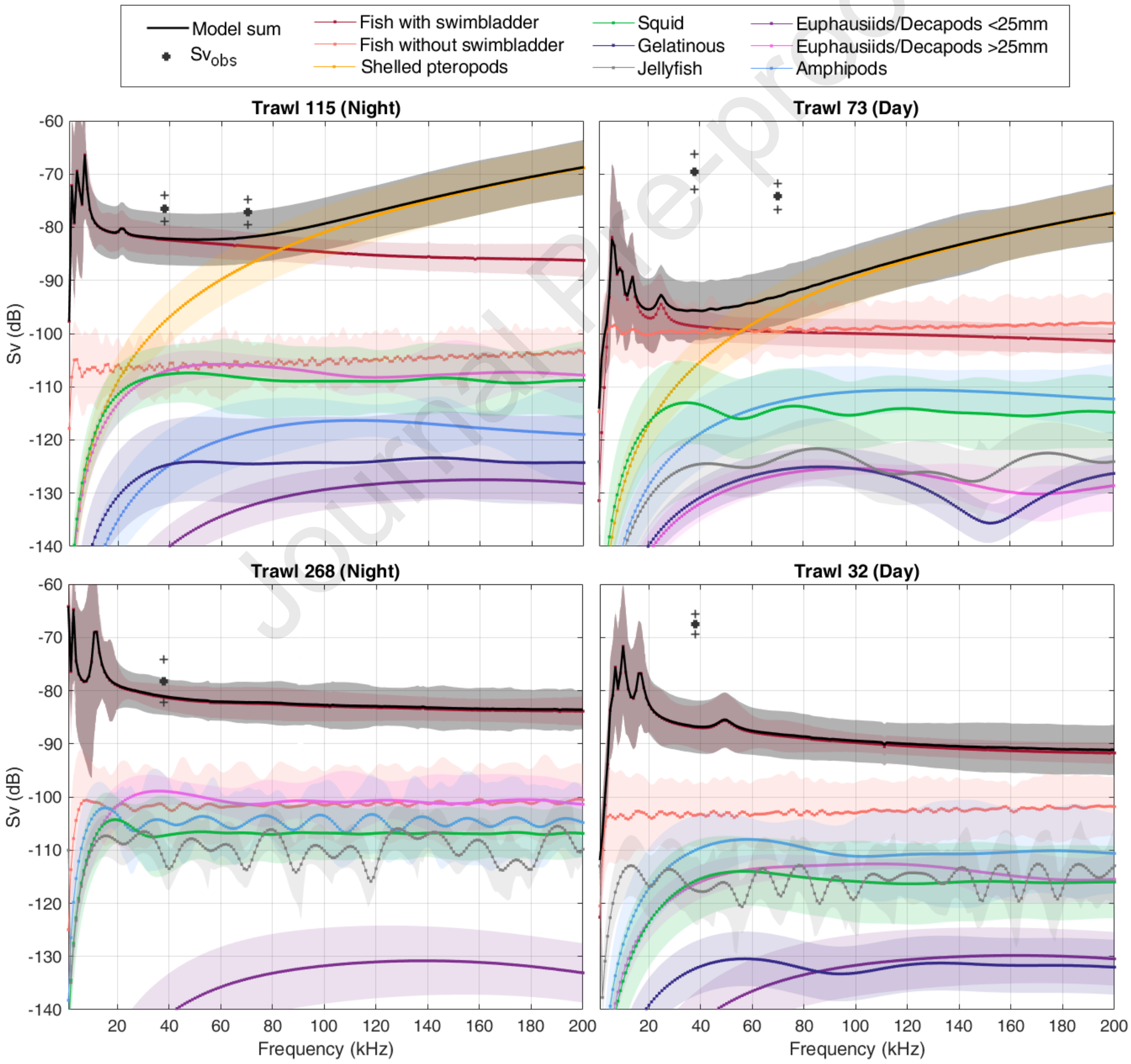

Figure 3. Forward modelling results for each category compared to the observed $S_{v,EK60}$ for four trawls: #115 (NEC5, d_{trawl}=169m), #268 (WARM, d_{trawl}=545m), #73 (NEC3, d_{trawl}=72m) and #32 (NEC2, d_{trawl}=509m). The modelled backscattering response $S_v(f)$ in dB re 1 m^{-1} of each acoustic category caught in the trawls are in coloured solid lines. The total modelled response $S_{v,mod}(f)$ summing the

contribution of all taxa is in solid black line. Shaded areas are the standard deviations of backscattering responses. In trawls #268 and #32, there is a partial overlap between the contribution of fish with swimbladders (red line) and $S_{v,mod}(f)$ (black line), and the response of fish with swimbladders is scarcely discernible. The *in situ* acoustic densities $S_{v,EK60}$ in *dB re 1 m^-1^* at 38 kHz and 70kHz are denoted by a black thick cross with their standard deviation in thin crosses. $S_{v,EK60}$ at 70kHz is only available for trawls at depths shallower than 400m.

1.4.1 Generalized Linear Model (GLM)

Generalized linear regression models (GLM) with Gaussian (identity-link) form were used to explore how $\Delta S_{v,f}$ was associated with the composition of trawls and the sampling characteristics. The predictor variables used in the GLM were: density of fish with swimbladders (ρ_{SWB}), density of crustaceans (sum of density of amphipod and euphausiid combined as ρ_{crust}), gelatinous density (sum of density of gelatinous and jellyfish as ρ_{gelat}), trawling depth (d_{trawl}) and relative weight of fish with swimbladders, crustaceans and gelatinous. The relative weights represented the measured weight of a taxa group (in g) over the total weight of the trawl. No collinearity among predictors was detected. After examining the distribution of densities, they were transformed into logarithmic scale, $\log 10(\rho)$, to better fit the residuals to a Normal distribution. The analysis was performed separately for 38 and 70kHz, and for day and night trawls (51 trawls for day and 93 at night) to better account for the impact of DVM (Casey and Myers, 1998). The best models were selected with the compensated Akaike Information Criteria (AICc; R package Mazerolle, 2023). The 4 optimal models (two for each frequency at both day and night-period) are presented in this study. Analyses were performed with R statistical software (R Core Team, 2023), version 4.3.1. Marginal effect plots showing the predicted $\Delta S_{v,f}$ for the significant variables (p-value<0.05) from the GLM models were plotted with the 'ggeffects' package (Lüdecke, 2018, version 1.2.2). The pseudo R-squared (R^2) of the models were determined with the McFadden (1973) metric.

2. Results

2.1 Biological sampling

Trawl sampling gathered a total number of 98,896 specimens, which represent a combination of different taxonomic levels including 306 species, 311 genus, 186 families and 55 orders (Table 2). The higher number of genera compared to species was a result of the inability to identify all specimen species due to their conservation state. Only 55% of the total specimens were determined at the species level, 8% at the genus level only, 30% at the family level, and 5% at the order level. Among the specimens that could not be identified at the species level, 58% were gelatinous organisms.

Myctophidae, Sternoptychidae and Gonostomatidae were the main fish families sampled. *Ceratoscopelus warmingii* was the most abundant species caught for fish with swimbladders. Fishes without swimbladder were mainly represented by Bathymyrinae subfamily (leptocephalus larval stage) and *Lobianchia gemellarii*. *Diaphus perspicillatus* presenting a gas-filled inclusion at the juvenile stage only was the most abundant species classified in both fish with or without swimbladder. Decapods and Euphausiids were mainly represented by *Thysanopoda* sp., *Euphausia mucronata* and *Janicella spinicauda*. Various species of the Phronimidae family, particularly *Phronima sedentaria*, and of the Phrosinidae family, including *Phrosina semilunata*, were collected within the amphipods taxa. Cephalopod specimens included *Pterygioteuthis* and *Abralia* genus. The family Bougainvilliidae represented most of the recognisable jellyfish samples while the gelatinous category contained predominantly *Pyrosoma* sp. and Salpidae. Families Agalmatidae and Physonectae represented most of the siphonophores with pneumatophores. Many gelatinous organisms caught in trawls were not sufficiently well preserved to accurately estimate their morphology and identify their species.

2.2 Forward approach $S_{v,mod}(f)$

When varying the input parameter values (Supplementary S3), the standard deviation of $S_{v,mod}(f)$ was +/- 5dB in average at 38 and 70 kHz (Figure 3). The resonance scattering region of gas-bearing organisms situated between 1 and 30 kHz exhibited the highest variability (+/- 10dB in average). The modelled results indicated that scatterers with fluid-like properties had a negligible impact on $S_{v,mod}$, which was dominated by the response of fish with swimbladders in the majority of trawls (Figure 3). When caught in trawls, elastic-shelled pteropods were the strongest scatterers at frequencies > 50-70kHz. In rare cases, some fluid-like categories had a density and a size distribution that led to a scattering response equal or higher than fish with swimbladders at f > 50kHz (e.g. Figure 3, Trawl 73). The response of the siphonophores with pneumatophore, the other gas-bearing organisms' category, did not have a major impact on $S_{v,mod}$.

2.3 Variability of $\Delta S_{v,f}$ across trawls

Across the 144 trawls, $\Delta S_{v,f}$ spanned a range of [-1.5, 42.1] dB at 38 kHz and [0.9, 42.4] dB at 70 kHz, with a median of 16 dB for the combined distribution of both frequencies. In trawls where d_{trawl} was less than 400m (within the maximum emission range of 70 kHz), $\Delta S_{v,38}$ and $\Delta S_{v,70}$ followed a linear regression (Figure 4a) with a slope of 0.96 (associated with a standard error of 0.03). This suggested that the variability of $\Delta S_{v,f}$ was consistent for both frequencies. $\Delta S_{v,f}$ was >0 (Figure 4b), indicating that the modelled volume backscatter $S_{v,mod}$ derived from trawl catch was lower than the observed $S_{v,obs}$ from the echosounder. Only two trawls, situated in the mesopelagic layer with d_{trawl}>200m, exhibited a $\Delta S_{v,38}$<0. On average, $\Delta S_{v,f}$ was higher during daytime trawls compared to night-time trawls for both frequencies, with median values of 19 dB and 22 dB for $\Delta S_{v38,day}$ and $\Delta S_{v70,day}$, and a median of 14 dB for $\Delta S_{v38,night}$ and $\Delta S_{v70,night}$ (Figure 4b).

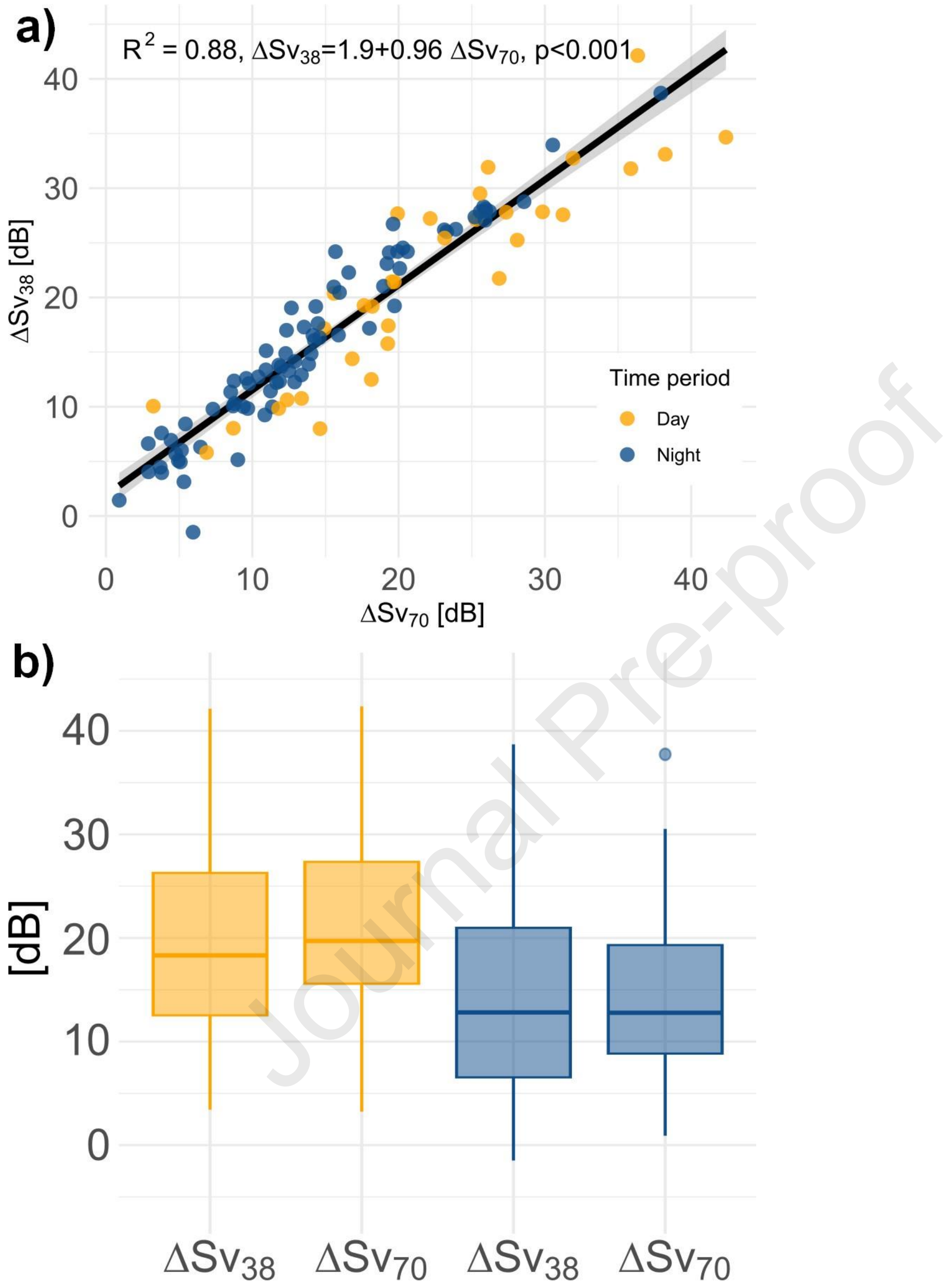

Figure 4. Description of $\Delta S_{v,f}$ in relation with time-period. (a) Relationship between ΔS_{v38} and ΔS_{v70} for each trawl with a linear regression fit (lm) in solid black line and the associated metrics (R^2, p-value and regression equation). Shaded areas represent 95% confidence interval. Dots represent each trawl with day in yellow and night in blue. (b) Summarized $\Delta S_{v,f}$ for day (yellow) and night (blue) trawls at 38 kHz (ΔS_{v38}) and 70 kHz (ΔS_{v70}). Horizontal line within each box is the median value, box limits are the inter-quartile range, i.e. 25 and 75% quantiles. The whiskers (vertical lines) are 1.5 times the inter-quartile range. Dots represent potential outliers.

2.4 Effect of organisms' density

The final models are displayed in Table 5, with only a single model for each day/night and frequency combination because the level of uncertainty in model structure was minimal (i.e., all other subsequent models had dAIC > 2, as shown in Supplementary Table S4). Out of all the predictors examined in the GLM, the log density of fish with swimbladders captured in trawls (log10(ρ_{SWB})), and the relative weight of fish with swimbladders (% weight fish SWB) were included in all four models selected with AICc, for both day and night trawls at 38 and 70kHz (Table 5). The predictor log10(ρ_{SWB}) was associated with a negative coefficient (Table 5), indicating that $\Delta S_{v,f}$ decreased in trawls with a high density of fish with swimbladders (Figure 5). $\Delta S_{v,f}$ also decreased with % weight fish SWB, in trawls where a large proportion of the sampled weight was represented by fish with swimbladders (Figure 5 and Table 5). Finally, the density of crustaceans, log10(ρ_{crust}), was included in the day-time GLM for $\Delta S_{v,70}$, with a negative coefficient indicating a decrease of $\Delta S_{v,70}$ in day-time trawls with a larger density of crustaceans at 70kHz.

2.5 Effect of trawling depth

The depth of trawls (d_{trawl}) was included in night-time models selected with AICc (Table 5). $\Delta S_{v,f}$ decreased in deeper trawls (Figure 5). The selected models explained around 80% of the variance of $\Delta S_{v,f}$ during the night and between 60 to 70% for day-time (Table 5). This finding highlighted that the models did not explain day-time discrepancies between trawl and acoustic observations to the same extent as they did in night-time scattering layers. The other predictors tested were not included in the selected GLM (Supplementary Table S4).

Focusing on the impact of depth, the distribution of $\Delta S_{v,f}$ was studied in two depth layers as in Figure 6: epipelagic ($d_{trawl} \leq$ 200m) and mesopelagic ([200, 800]m for 38 kHz and [200, 400] for 70kHz) layers. $\Delta S_{v,f}$ was lower in the mesopelagic layer for both frequencies with a minimum at night (median $\Delta S_{v,f}$ of 3.9 and 5.0 dB, for 38 and 70 kHz, respectively), at the exception of day-time 70kHz. 90% of $\Delta S_{v,38} \leq$ 5dB (15 trawls) were located in the night-time mesopelagic layer, which is the scattering layer with the least average difference between $S_{v,mod}$ and $S_{v,obs}$ (Figure 4).

Table 5. GLM's results for the 4 final models (rows) selected based on the lowest AICc (see Table S3 for full model selection outputs). The response variables ΔS_{v38} and ΔS_{v70} are modelled separately and are split into day/night trawls. The proportion of variance explained (R^2), the beta-coefficients from the GLM of the predictor variables in each model and their standard errors (STD) are indicated for each model. Predictor variables are depth (d_{trawl}), density of fish with swimbladders in logarithmic scale (log10(ρ_{SWB})), relative weight of fish with swimbladders (% weight fish SWB) and density of

crustaceans in logarithmic scale ($log10(\rho_{crust})$). Blank cases indicate the variables not included in the GLM selected with AICc criteria. All predictors are associated to a p-value<0.05.

$\Delta S_{v,f}$ (kHz)	Period	R^2	$log10(\rho_{Fish\ SWB})$ (STD)	% weight fish SWB (STD)	d_{trawl} (STD)	$log10(\rho_{crust})$ (STD)
38	Day	62%	-6 (1)	-9 (5)		
70	Day	73%	-6 (1)	-15 (6)		-4 (2)
38	Night	80%	-6 (1)	-8 (2)	-0.03 (0.007)	
70	Night	78%	-6 (1)	-6 (2)	-0.04 (0.007)	

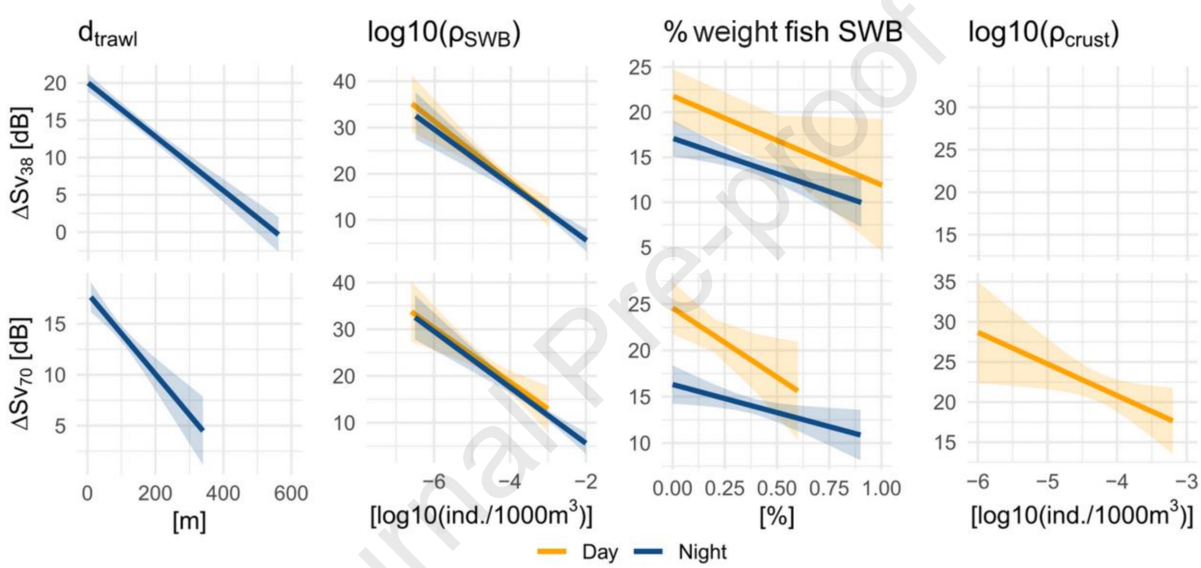

Figure 5. Predicted marginal effects of $\Delta S_{v,f}$ for the 4 GLM models as a function of predictors. $\Delta S_{v,38}$ (top) and $\Delta S_{v,70}$ (bottom) predicted for day (yellow solid line) and night (blue solid line) models for the variables d_{trawl}, $log10(\rho_{SWB})$, % weight fish SWB and $log10(\rho_{crust})$. Shaded areas represent 95% confidence interval of marginal effects. Only the variables selected in the 4 GLM models and presented in Table 5 are plotted. They are all associated to a p-value<0.05.

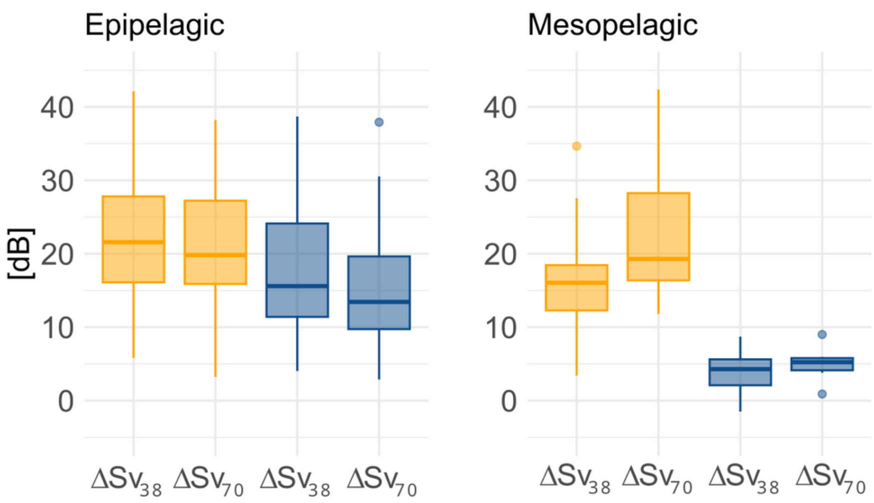

Figure 6. Description of $\Delta S_{v,f}$ distributions per depth layers and time-period: $\Delta S_{v,f}$ in the epipelagic layer (left, d_{trawl} ≤200m) and in the mesopelagic layer (right, d_{trawl}>200m) at 38 kHz (ΔS_{v38}) and 70 kHz (ΔS_{v70}) for day (yellow) and night (blue) trawls. Horizontal line within each box is the median value, box limits are the inter-quartile range, i.e. 25 and 75% quantiles. The whiskers (vertical lines) are 1.5 times the inter-quartile range. Dots represent potential outliers.

3. Discussion

Using 144 trawls between the surface and 600m depth, along with 38 and 70 kHz acoustics covering a 10-years period in West tropical Pacific, this study provides information on how acoustic-trawl estimates vary in tropical ecosystems characterized by high biodiversity. The backscattering difference $\Delta S_{v,f}$ between the observed and the predicted acoustic signal using forward modelling was function of the time period (day/night) and decreased with larger weight ratio and density of fish with swimbladders at 38 and 70kHz. In addition, $\Delta S_{v,70}$ during day-time also decreased with the increasing density of crustaceans. The towing depth of each trawl had an effect on $\Delta S_{v,f}$ during the night, with a significantly smaller difference in mesopelagic than epipelagic trawls. These observations show that the interpretation of acoustic-trawl survey results depends on spatial and temporal patterns and is therefore sensitive to the choice of sampling depth and survey time-period (day/night). The values of $\Delta S_{v,f}$ were positive over the entire dataset showing a modelled S_v lower than observed with echosounder value. This consistent positive bias may be linked to an overestimation with hull-mounted echosounders and/or an underestimation of volume backscattering in forward modelling, either due to the models parameterisation or biases in the species diversity and abundance sampled with the trawl (Mair et al., 2005; Blanluet et al., 2019).

3.1 Uncertainties due to acoustics

The predicted acoustic signal $S_{v,mod}$ depends on the model parameter values and the species composition (diversity and relative abundances) observed in the trawl samples. The incoherent summation of organism contributions relies on the assumption that the backscatter of individual organisms is not affected by neighboring ones, and that their distribution is random within the observed volume. The low densities observed in this study and the mixed nature of the scattering layers allowed us to make this assumption. However, this commonly accepted approach remains simplified and may introduce significant uncertainty into $S_{v,mod}$. The model parameters were chosen from the literature, but were not specific to the tropical Pacific area nor to all taxa caught in trawls, which introduced another source of uncertainty (Lawson et al., 2004, Lucca et al., 2021). $S_{v,mod}$ modelled with the parameters chosen in this study was defined as the reference value for all analysis. However, the selection of input parameters for the backscattering models of each taxon group (Table 3 and 4) introduced variability in the modelled backscattering response. Model uncertainty analysis indicated that the total volume backscatter could vary within +/-5dB around the reference value of $S_{v,mod}$ at 38 and 70 kHz, solely as a function of input parameters (Figure 3). In trawls where $\Delta S_{v,f} \leq$ 5dB, predominantly located in the night-time mesopelagic layer, the variability in total modelled backscatter could solely account for the disparity between $S_{v,mod}$ and $S_{v,obs}$. For all other cases, where the median $\Delta S_{v,f}$ was larger than 5 dB, the uncertainty associated with model parameters alone could not explain these differences.

As expected, at 38 and 70kHz, $S_{v,mod}$ was primarily dominated by the response of fish with swimbladders, making this group essential for modelling the trawl's backscatter (McClatchie et al., 2000; Kloser et al., 2009; Davison et al., 2015). Among all the parameters for this gas-bearing scattering group, the parameters controlling the swimbladder volume and shape, which vary significantly between species, generated the highest sensitivity on the modelled volume backscatter, as also shown in Proud et al. (2019). Yet assess these parameters for all specimens often require dissection and X-ray or CT-scan to evaluate their variability within species and establish a relation with fish length (Yasuma et al., 2010). These methods are performed only on undamaged specimens with preferably intact swimbladders. However, when bringing mesopelagic fish to the surface, the swimbladder experiences a rapid pressure change during ascent, raising uncertainties regarding whether its morphology and volume remain identical to those in deep layers (Sobradillo et al., 2019; Peña et al., 2023; Sarmiento-Lezcano et al., 2023). For all these reasons, many taxa do not yet have a description regarding the presence of a swimbladder. Choosing to assign them a swimbladder characteristic identical to that of specimens from the same family, to avoid excluding them from the study, introduces a source of error in the modelling (Dornan et al., 2019; Marohn et al., 2021).

The group of elastic-shelled pteropods can occasionally dominate the volume backscatter at 70 kHz frequency. Their solid shells tend to produce a strong backscattering response even at low densities when compared to fluid-like animals (Stanton et al., 1994). This strong response was computed by a high-pass dense fluid-sphere with an empirical reflection coefficient from Stanton, (1994) which is often used in studies (Lawson et al., 2004; Lavery et al., 2007; Blanluet et al., 2019). This model is relatively simple and does not represent shelled-pteropods that exhibit more complex shapes (spirals or pyramidal shell as *Clio pyramidata* and an opercular opening) and various materials (aragonite, calcite or silica). This assumption might overestimate the actual backscatter. Better knowledge is also required on the scattering responses of gelatinous organisms such as salps and pyrosomes and more broadly of a large range of more rare species (Warren and Smith, 2007; Henschke et al., 2016).

During the day, the 70 kHz signal was more sensitive to the density of crustaceans as $\Delta S_{v,70}$ decreased with larger densities. Recording acoustic data at higher frequencies (120 and 200 kHz) would help to estimate the effect of the groups of crustaceans and fluid-like organisms (gelatinous, squids and jellyfishes) in the upper layer as suggested in other studies (e.g., Jech et al., 2018; Lucca et al., 2021) as they are further away from the resonance frequencies of gas-filled structures often situated between 18 and 70 kHz. At these higher frequencies, the relationship between volume backscatter and biomass becomes more linear as proposed in Benoit-Bird, (2009). However, the data at 120 and 200 kHz in our surveys were of bad quality. Therefore, our findings likely depict trends related to gas-bearing mesopelagic fishes.

3.2 Micronekton trawl sampling

The large $\Delta S_{v,f}$ can also be linked to the underestimation of abundance and biases in the species composition as caught by the trawl sampling. Utilizing forward modelling on biological sampling necessitates precise estimates of the abundance, weight, size distribution, and morphological characteristics of the groups of species defined in the model to accurately calculate the theoretical mean volume backscatter in a specific sampled layer. However, the tropical Pacific Ocean has a very high species diversity with potentially strong spatial heterogeneity in the horizontal and vertical distributions of species, making it difficult to achieve comprehensive trawl sampling.

Trawl catchability is a function of its design and operational features (i.e., length, mesh size, trawl opening and towing speed) and the characteristics of the organisms captured (i.e., swimming speed, length and shape; Grimaldo et al., 2022). Some organisms tend to avoid the trawl or escape it after entering, with their chance of escaping the trawl increasing with the swimming speed (Bethke et al., 1999; De Robertis et al., 2017a; Grimaldo et al., 2022). With trawls towed around 2 to 3 knots (as in this study), fast swimming species in mesopelagic fishes and squids (Peña et al., 2018) can likely escape or stay away from the trawl (Kaartvedt et al., 2012; Davison et al., 2015; Underwood et al., 2020). Increasing the towing speed would potentially reduce the avoidance factor but is not conceivable with all vessels and/or all trawls. The avoidance factor may be more pronounced in the surface layers where organisms might detect the approaching trawl due to sunlight during the day and artificial lights from the vessel during the night (Pakhomov and Yamamura, 2010). Thus, the largest differences of $\Delta S_{v,f}$ in the epipelagic layer might, in part, be attributed to the influence of light leading to lower catchability.

In addition, the mesh-size selectivity, is also important in the trawl-based estimates of micronekton biomass. The size selectivity leads to an incomplete length distribution of micronekton specimen (Lawson et al., 2004; Proud et al., 2019). The net in our study presenting a graded mesh, all taxa may not be herded by the largest mesh (80mm) at the entrance nor gathered homogeneously down to the cod-end (Heino et al., 2011; De Robertis et al., 2017a). The smallest and least mobile micronekton organisms, mainly crustaceans, gelatinous and shelled-pteropods, may pass through the largest mesh to be captured only in the narrowest mesh at the end of the trawl (Kloser et al., 2009). This selectivity would affect the determination of the effective opening surface utilized to estimate the sampling volume and introduce a correlation with the size distribution of organisms. The replication of tows at one station for the same scattering layer would reduce the variability in length distribution and help assess the size selectivity (Lawson et al., 2004).

Underestimation of mesopelagic fish cannot explain alone the variability of $\Delta S_{v,f}$. Large differences ($\Delta S_{v,f}$>15 dB) were observed in all depth layers and time-period at the exception of night-time mesopelagic layer. They were not systematically associated with a low density of fish with swimbladders (relatively compared to the other micronektonic densities). In those cases, ρ_{SWB} alone could not explain the variability of $\Delta S_{v,f}$ indicating that i) acoustic backscatter was due to other species not sampled by the trawl (i.e. possibly siphonophores with pneumatophores), and/or ii) the acoustic theoretical response of the present specimens was not properly modelled. Gelatinous organisms in particular are sensitive to both aspects, because they are fragile and their acoustic response is poorly known. The trawl used in this study is not well suited to collect jellyfish and gelatinous colonial organisms (salps, siphonophores). Those that end up in the cod-end are often brought aboard broken or damaged, which renders their counting and morphological description difficult. Siphonophores can contribute significantly to the mean volume backscattering strength and generate a signal as strong as mesopelagic fish in total mesopelagic backscatter (Proud et al., 2019) with a consequent impact on biomass estimates (Blanluet et al., 2019, Proud et al., 2019). In this study, siphonophores were caught in few trawls (only 3%) and their abundance might have been underestimated because of the difficulty to catch fragile colonial organisms in trawls. Their abundance and length remain largely unknown in open ocean (Kloser et al., 2016). Pneumatophores have been reported to a length ranging from 0.05

to 1.5 mm (Benfield et al., 2003; Lavery et al., 2007; Kloser et al., 2016) and the importance of the contribution of their fluid-like parts (bracts and nectophores) is still debated (Lavery et al., 2007), which makes their inclusion in forward problem complex in the absence of precise observations.

Supplementing trawl sampling with nets designed for capturing smaller species and zooplankton, such as the Methot Isaac Kidd and/or the Multinet (Blanluet et al., 2019), could enhance the identification and abundance estimates of gelatinous and other fragile, smaller organisms. Zooplankton and small organisms can form dense aggregations and sometimes contribute to more than 50% of backscattering, as observed at 120kHz with copepods in Lawson et al. (2004). Overall, despite the use of all sampled taxa in this study to take into account the diversity of micronekton organisms, our results are focused on mesopelagic fish with swimbladders abundance estimates.

3.4 Variability of observed scattering layers

The spatial organization of scattering layers plays a role in the variability of $\Delta S_{v,f}$. In our model, scattering layers were considered homogenous all along the tows. However, that this is not necessarily true (Benoit-Bird et al., 2017). Patchy distributions and small schools were often observed on the echosounder data, especially in surface layers. These aggregations have a strong acoustic response but are not homogeneously distributed and may have been missed by our trawl, explaining discrepancies between sampling methods with a strong acoustics observation not found in trawl samples (Lawson et al., 2004). Clustering algorithms seem to make it possible to differentiate sublayers that are inhomogeneous from an acoustic point of view (Blanluet et al., 2019). Taking into account these different strata could help understand which areas have been better sampled by the trawl. This can be achieved by modelling the acoustic response based on micronektonic compositions and comparing it to the signal from different sub-layers, instead of relying on the averaged backscatter of a single large scattering layer.

3.4 Perspectives and complementary sampling methods

To progress in our understanding of the relationships between hull-mounted acoustic data and trawl sampling data, complementary approaches are needed to improve species identification and individual abundance estimates. Optical devices are a promising tool to identify species, measure and count organisms, either independently (Williams et al., 2018; Gastauer et al., 2022) or in conjunction with another measurement method, such as using them on a trawl to document organisms entering the net (Allken et al., 2021) or an acoustic probe (Marouchos et al., 2016). Infrared stereo-camera profiles down to 150m depth in nearshore stations have been used to estimate the sizes and densities of micronekton in scattering layers (Benoit-Bird, 2009). These data showed a correlation between the densities of micronekton (mainly myctophids without gas-swimbladder) and volume scattering from echosounders. However, optical measurements in deep scattering layers require the use of a light source that might affect the behaviour of the organisms. Peña et al. (2020), Geoffroy et al. (2021) and Underwood et al. (2021) highlighted the change in behaviour of organisms to an artificial light source, with clear avoidance of mesopelagic fish in white light. Uncertainty remains about the impact of other colours and the wavelength used, but it could introduce another set of biases to biomass estimates.

Acoustic profilers or probes submerged in mesopelagic layers appear to be a possible approach linking trawls and acoustics (Kloser et al., 2016). Given the limited range of emission of hull-mounted sounders at high frequencies, vertical profilers using frequencies higher than 70 kHz would be useful. Wideband acoustic profilers in particular, presenting a high-resolution and a smaller insonified volume than hull-mounted echosounder in deep layers, offer a better chance at detecting individual targets (Bassett et al., 2020; Cotter et al., 2021). Weak, fluid-like scatterers are not masked by gas-filled organisms in the small sampled volume and are therefore detectable with echo-counting algorithms to estimate their density (Agersted et al., 2021a; Cotter et al., 2021). To study scattering layers with trawls and profiler simultaneously, a solution would be to add the wideband profiler on the pelagic trawl opening to record organisms in front of it as in Underwood et al. (2020). This setup detect the behaviour of the organisms in front of the trawl and is a useful tool to calculate the avoidance and escapement rate of a trawl. The question of what organisms are actually detected with the profiler remains when estimating biomass. To accurately compute the total backscatter, it is essential to determine the proportion and exact acoustic response of each taxa across a wide frequency band, as opposed to relying solely on the response at discrete frequencies (Proud et al., 2019). The wideband properties allow us to study the detected targets response as a function of frequency band. Using this information is the next step to better understand the composition of mixed scattering layers by classifying the different target responses as in Verma et al. (2017) and Agersted et al. (2021b) and link them with broad taxa groups. We are currently systematically associating such wideband profiler to sampling trawl to assist in the correction of collected density of organisms when quantifying biomass. Finally, it seems that techniques based on environmental DNA could complement the trawl sampling to obtain key information on species composition and even rough estimate of abundance by taxa (Bessey et al., 2021; Govindarajan et al., 2022, 2023; Albonetti et al., 2023).

3.5 Concluding remarks

The comparison of micronekton density in acoustic-trawl surveys has highlighted significant disparities in organism abundance in tropical ecosystems defined by a high biodiversity. It showed the relationship between these differences with depth, time-period and composition of the trawl. Even when including all categories of micronekton scatterers, our acoustic-trawl surveys favoured the estimation of the density of mesopelagic fish; a result common to most mesopelagic studies at 38kHz (Scoulding et al., 2015; Proud et al., 2019; Dornan et al., 2022). In this study, the mesopelagic layer, especially at night, displays the smallest divergence between acoustics and trawl. In this case, it is recommended to initially focus on this layer for estimating mesopelagic biomass. This layer shows the most consistent results between the two methods, making them easier to interpret.

Finally, it is obvious that the sampling of micronekton should be conducted concurrently using a combination of methods, including hull-mounted echosounders, towed probes employing acoustics and optics, alongside trawl samplings and genomics. Validating acoustic measurements with other methods would help understanding and reducing the large differences between acoustics and trawl sampling to improve abundance and biomass estimates of micronekton in tropical pelagic ecosystems.

Acknowledgements

The authors thank the two reviewers for their valuable comments to improve the manuscript. We thank the crew and officers of R/V ALIS for their help and cooperation and scientists who took part in the cruises. We express our sincere thanks to J. Potts (SPC) for her assistance and guidance with statistics analysis. We are grateful to the WCPFC Pacific Marine Specimen Bank and the Pacific Community (SPC), Fisheries, Aquaculture and Marine Ecosystems (FAME) division for collating and providing quantitative and qualitative information on micronekton species composition. We are grateful to P. Machful for her valuable contributions to the swimbladders references. This work results from a collaborative work between SPC and IRD and was co-funded by the BEST 2.0 Programme funded by the European Union (project BIOPELAGOS), the French national program LEFE/INSU, French Pacific Fund, the French Ministry of Armies, IRD and SPC. We thank K. Olu from Ifremer co-leader with V. Allain of the cruise KANARECUP. Oceanographic ships are provided by the French Oceanographic Fleet. Laure Barbin's doctoral grant was funded by Sorbonne Université. This work benefited from the work done and the exchanges within the ICES WGFAST community.

Authors contributions

Laure Barbin: Conceptualization, methodology, formal analysis, writing original draft, writing review and editing ; Anne Lebourges-Dhaussy: Conceptualization, writing review and editing ; Valérie Allain: Project administration, writing review and editing ; Aurore Receveur: Conceptualization, writing review and editing, formal analysis ; Patrick Lehodey: Conceptualization, writing review and editing ; Jérémie Habasque : writing review and editing ; Elodie Vourey : Data Curation, Validation ; Annie Portal : Data Curation; Gildas Roudaut : Data Curation ; Christophe Menkes: Conceptualization, Project administration, writing review and editing.

References

Agersted, M.D., Khodabandeloo, B., Klevjer, T.A., García-Seoane, E., Strand, E., Underwood, M.J., Melle, W., 2021a. Mass estimates of individual gas-bearing mesopelagic fish from *in situ* wideband acoustic measurements ground-truthed by biological net sampling. ICES Journal of Marine Science 78, 3658–3673. https://doi.org/10.1093/icesjms/fsab207

Agersted, M.D., Khodabandeloo, B., Liu, Y., Melle, W., Klevjer, T.A., 2021b. Application of an unsupervised clustering algorithm on *in situ* broadband acoustic data to identify different mesopelagic target types. ICES Journal of Marine Science 78, 2907–2921. https://doi.org/10.1093/icesjms/fsab167

Albonetti, L., Maiello, G., Cariani, A., Carpentieri, P., Ferrari, A., Sbrana, A., Shum, P., Talarico, L., Russo, T., Mariani, S., 2023. DNA metabarcoding of trawling bycatch reveals diversity and distribution patterns of sharks and rays in the central Tyrrhenian Sea. ICES Journal of Marine Science 80, 664–674. https://doi.org/10.1093/icesjms/fsad022

Allain, V., Menkes, C., 2018. WALLALIS cruise, Alis R/V. https://doi.org/10.17600/18000523

Allain, V., Menkes, C., 2016. NECTALIS-5 cruise, Alis R/V. https://doi.org/10.17600/16004200

Allain, V., Menkes, C., 2015. NECTALIS-4 cruise, Alis R/V. https://doi.org/10.17600/15004000

Allain, V., Menkes, C., 2014. NECTALIS-3 cruise, Alis R/V. https://doi.org/10.17600/14004900

Allain, V., Menkes, C., 2011a. NECTALIS-1 cruise, Alis R/V. https://doi.org/10.17600/11100050

Allain, V., Menkes, C., 2011b. NECTALIS-2 cruise, Alis R/V. https://doi.org/10.17600/11100070

Allken, V., Rosen, S., Handegard, N.O., Malde, K., 2021. A deep learning-based method to identify and count pelagic and mesopelagic fishes from trawl camera images. ICES Journal of Marine Science 78, 3780–3792. https://doi.org/10.1093/icesjms/fsab227

Anderson, T.R., Martin, A.P., Lampitt, R.S., Trueman, C.N., Henson, S.A., Mayor, D.J., 2019. Quantifying carbon fluxes from primary production to mesopelagic fish using a simple food web model. ICES Journal of Marine Science 76, 690–701. https://doi.org/10.1093/icesjms/fsx234

Anderson, V.C., 1950. Sound scattering from a fluid sphere. The Journal of the Acoustical Society of America 22, 426–431. https://doi.org/10.1121/1.1906621

Ariza, A., Garijo, J.C., Landeira, J.M., Bordes, F., Hernández-León, S., 2015. Migrant biomass and respiratory carbon flux by zooplankton and micronekton in the subtropical northeast Atlantic Ocean (Canary Islands). Progress in Oceanography 134, 330–342. https://doi.org/10.1016/j.pocean.2015.03.003

Ariza, A., Lengaigne, M., Menkes, C., Lebourges-Dhaussy, A., Receveur, A., Gorgues, T., Habasque, J., Gutiérrez, M., Maury, O., Bertrand, A., 2022. Global decline of pelagic fauna in a warmer ocean. Nature Climate Change 12, 928–934. https://doi.org/10.1038/s41558-022-01479-2

Arreguín-Sánchez, F., 1996. Catchability: a key parameter for fish stock assessment. Reviews in Fish Biology and Fisheries volume 6, 22. https://doi.org/10.1007/BF00182344

Bassett, C., Lavery, A.C., Stanton, T.K., Cotter, E.D., 2020. Frequency- and depth-dependent target strength measurements of individual mesopelagic scatterers. The Journal of the Acoustical Society of America 148, EL153–EL158. https://doi.org/10.1121/10.0001745

Benfield, M.C., Lavery, A.C., Wiebe, P.H., Greene, C.H., Stanton, T.K., Copley, N.J., 2003. Distributions of physonect siphonulae in the Gulf of Maine and their potential as important sources of acoustic scattering. Canadian Journal of Fisheries and Aquatic Sciences 60, 14. https://doi.org/10.1139/f03-065

Benoit-Bird, K.J., 2009. The effects of scattering-layer composition, animal size, and numerical density on the frequency response of volume backscatter. ICES Journal of Marine Science 66, 582–593. https://doi.org/10.1093/icesjms/fsp013

Benoit-Bird, K.J., Lawson, G.L., 2016. Ecological insights from pelagic habitats acquired using active acoustic techniques. Annual Review of Marine Science 8, 463–490. https://doi.org/10.1146/annurev-marine-122414-034001

Benoit-Bird, K.J., Moline, M.A., Southall, B.L., 2017. Prey in oceanic sound scattering layers organize to get a little help from their friends. Limnology and Oceanography 62, 2788–2798. https://doi.org/10.1002/lno.10606

Bertrand, A., Bard, F.-X., Josse, E., 2002. Tuna food habits related to the micronekton distribution in French Polynesia. Marine Biology 140, 1023–1037. https://doi.org/10.1007/s00227-001-0776-3

Bessey, C., Neil Jarman, S., Simpson, T., Miller, H., Stewart, T., Kenneth Keesing, J., Berry, O., 2021. Passive eDNA collection enhances aquatic biodiversity analysis. Communications Biology 4, 236. https://doi.org/10.1038/s42003-021-01760-8

Bethke, E., Arrhenius, F., Cardinale, M., Håkansson, N., 1999. Comparison of the selectivity of three pelagic sampling trawls in a hydroacoustic survey. Fisheries Research 44, 15–23. https://doi.org/10.1016/S0165-7836(99)00054-5

Blackburn, M., 1968. Micronekton of the eastern tropical Pacific Ocean: Family composition, distribution, abundance, and relations to tuna. Fisheries Bulletin US 67, 71–115.

Blanluet, A., Doray, M., Berger, L., Romagnan, J.-B., Le Bouffant, N., Lehuta, S., Petitgas, P., 2019. Characterization of sound scattering layers in the Bay of Biscay using broadband acoustics, nets and video. PLoS ONE 14, e0223618. https://doi.org/10.1371/journal.pone.0223618

Brierley, A.S., 2014. Diel vertical migration. Current Biology 24, R1074–R1076. https://doi.org/10.1016/j.cub.2014.08.054

Brodeur, R.D., Seki, M.P., Pakhomov, E.A., Suntsov, A.V., 2004. Micronekton - What are they and why are they important? PICES Press 13, 7–11.

Burgos, J.M., Horne, J.K., 2008. Characterization and classification of acoustically detected fish spatial distributions. ICES Journal of Marine Science 65, 1235–1247. https://doi.org/10.1093/icesjms/fsn087

Casey, J.M., Myers, R.A., 1998. Diel variation in trawl catchability: is it as clear as day and night? Canadian Journal of Fisheries and Aquatic Sciences 55, 2329–2340.

Cotter, E., Bassett, C., Lavery, A., 2021. Comparison of mesopelagic organism abundance estimates using *in situ* target strength measurements and echo-counting techniques. JASA Express Letters 1, 040801. https://doi.org/10.1121/10.0003940

Czudaj, S., Koppelmann, R., Möllmann, C., Schaber, M., Fock, H.O., 2021. Community structure of mesopelagic fishes constituting sound scattering layers in the eastern tropical North Atlantic. Journal of Marine Systems 224, 103635. https://doi.org/10.1016/j.jmarsys.2021.103635

Davison, P.C., Checkley, D.M., Koslow, J.A., Barlow, J., 2013. Carbon export mediated by mesopelagic fishes in the northeast Pacific Ocean. Progress in Oceanography 116, 14–30. https://doi.org/10.1016/j.pocean.2013.05.013

Davison, P.C., Koslow, J.A., Kloser, R.J., 2015. Acoustic biomass estimation of mesopelagic fish: backscattering from individuals, populations, and communities. ICES Journal of Marine Science 72, 1413–1424. https://doi.org/10.1093/icesjms/fsv023

De Robertis, A., Taylor, K., Williams, K., Wilson, C.D., 2017a. Species and size selectivity of two midwater trawls used in an acoustic survey of the Alaska Arctic. Deep Sea Research Part II: Topical Studies in Oceanography 135, 40–50. https://doi.org/10.1016/j.dsr2.2015.11.014

De Robertis, A., Taylor, K., Wilson, C.D., Farley, E.V., 2017b. Abundance and distribution of Arctic cod (*Boreogadus saida*) and other pelagic fishes over the U.S. Continental Shelf of the Northern Bering and Chukchi Seas. Deep Sea Research Part II: Topical Studies in Oceanography 135, 51–65. https://doi.org/10.1016/j.dsr2.2016.03.002

Demer, D.A., Berger, L., Bernasconi, M., Bethke, E., Boswell, K.M., Chu, D., Domokos, R., Dunford, A., Fassler, S., Gauthier, S., Hufnagle, L. T., Jech, J. M., Bouffant, N., Lebourges-Dhaussy, A., Lurton, X., Macaulay, G. J., Perrot, Y., Ryan, T., Parker-Stetter, S., Stienessen, S., Weber, T., Williamson, N., 2015. Calibration of acoustic instruments. ICES Cooperative Research Report 326, 133. http://dx.doi.org/10.25607/OBP-185

Dornan, T., Fielding, S., Saunders, R.A., Genner, M.J., 2022. Large mesopelagic fish biomass in the Southern Ocean resolved by acoustic properties. Proceedings of the Royal Society B: Biological Sciences 289, 20211781. https://doi.org/10.1098/rspb.2021.1781
Dornan, T., Fielding, S., Saunders, R.A., Genner, M.J., 2019. Swimbladder morphology masks Southern Ocean mesopelagic fish biomass. Proceedings of the Royal Society B: Biological Sciences 286, 20190353. https://doi.org/10.1098/rspb.2019.0353
Escobar-Flores, P.C., Ladroit, Y., O'Driscoll, R.L., 2019. Acoustic assessment of the micronekton community on the Chatham Rise, New Zealand, using a semi-automated approach. Frontiers in Marine Science 6, 507. https://doi.org/10.3389/fmars.2019.00507
Fjeld, K., Tiller, R., Grimaldo, E., Grimsmo, L., Standal, I.-B., 2023. Mesopelagics–New gold rush or castle in the sky? Marine Policy 147, 105359. https://doi.org/10.1016/j.marpol.2022.105359
Foote, K.G., 1983. Linearity of fisheries acoustics, with addition theorems. The Journal of the Acoustical Society of America 73, 1932–1940. https://doi.org/10.1121/1.389583
Foote, K.G., Knudsen, H.P., Vestnes, G., MacLennan, D.N., Simmonds, E.J., 1987. Calibration of acoustic instruments for fish density estimation: A practical guide. ICES Cooperative Research Reports (CRR). https://doi.org/10.17895/ices.pub.8265
Gastauer, S., Nickels, C.F., Ohman, M.D., 2022. Body size- and season-dependent diel vertical migration of mesozooplankton resolved acoustically in the San Diego Trough. Limnology & Oceanography 67, 300–313. https://doi.org/10.1002/lno.11993
Geoffroy, M., Langbehn, T., Priou, P., Varpe, Ø., Johnsen, G., Le Bris, A., Fisher, J.A.D., Daase, M., McKee, D., Cohen, J., Berge, J., 2021. Pelagic organisms avoid white, blue, and red artificial light from scientific instruments. Scientific Reports 11, 14941. https://doi.org/10.1038/s41598-021-94355-6
Gjøsæter, J., Kawaguchi, K., 1980. A review of the world resources of mesopelagic fish. FAO Fisheries Technical Paper.
Govindarajan, A.F., Llopiz, J.K., Caiger, P.E., Jech, J.M., Lavery, A.C., McMonagle, H., Wiebe, P.H., Zhang, W. (Gordon), 2023. Assessing mesopelagic fish diversity and diel vertical migration with environmental DNA. Front. Mar. Sci. 10, 1219993. https://doi.org/10.3389/fmars.2023.1219993
Govindarajan, A.F., McCartin, L., Adams, A., Allan, E., Belani, A., Francolini, R., Fujii, J., Gomez-Ibañez, D., Kukulya, A., Marin, F., Tradd, K., Yoerger, D.R., McDermott, J.M., Herrera, S., 2022. Improved biodiversity detection using a large-volume environmental DNA sampler with in situ filtration and implications for marine eDNA sampling strategies. Deep Sea Research Part I: Oceanographic Research Papers 189, 103871. https://doi.org/10.1016/j.dsr.2022.103871
Grimaldo, E., Herrmann, B., Brčić, J., Cerbule, K., Brinkhof, J., Grimsmo, L., Jacques, N., 2022. Prediction of potential net panel selectivity in mesopelagic trawls. Ocean Engineering 260, 111964. https://doi.org/10.1016/j.oceaneng.2022.111964
Heino, M., Porteiro, F.M., Sutton, T.T., Falkenhaug, T., Godø, O.R., Piatkowski, U., 2011. Catchability of pelagic trawls for sampling deep-living nekton in the mid-North Atlantic. ICES Journal of Marine Science 68, 377–389. https://doi.org/10.1093/icesjms/fsq089
Henschke, N., Everett, J.D., Richardson, A.J., Suthers, I.M., 2016. Rethinking the Role of Salps in the Ocean. Trends in Ecology & Evolution 31, 720–733. https://doi.org/10.1016/j.tree.2016.06.007
Hidalgo, M., Browman, H.I., 2019. Developing the knowledge base needed to sustainably manage mesopelagic resources. ICES Journal of Marine Science 76, 609–615. https://doi.org/10.1093/icesjms/fsz067
Hill Cruz, M., Kriest, I., Getzlaff, J., 2023. Diving deeper: Mesopelagic fish biomass estimates comparison using two different models. Front. Mar. Sci. 10, 1121569. https://doi.org/10.3389/fmars.2023.1121569
Jech, J.M., Horne, J.K., Chu, D., Demer, D.A., Francis, D.T.I., Gorska, N., Jones, B., Lavery, A.C., Stanton, T.K., Macaulay, G.J., Reeder, D.B., Sawada, K., 2015. Comparisons among ten models

of acoustic backscattering used in aquatic ecosystem research. The Journal of the Acoustical Society of America 138, 3742–3764. https://doi.org/10.1121/1.4937607

Jech, J.M., Lawson, G.L., Lowe, M.R., 2018. Comparing acoustic classification methods to estimate krill biomass in the Georges Bank region from 1999 to 2012: Georges Bank krill biomass. Limnology and Oceanography: Methods 16, 680–695. https://doi.org/10.1002/lom3.10275

Jones, B.A., Lavery, A.C., Stanton, T.K., 2009. Use of the distorted wave Born approximation to predict scattering by inhomogeneous objects: Application to squid. The Journal of the Acoustical Society of America 125, 73–88. https://doi.org/10.1121/1.3021298

Kaartvedt, S., Staby, A., Aksnes, D., 2012. Efficient trawl avoidance by mesopelagic fishes causes large underestimation of their biomass. Marine Ecology Progress Series 456, 1–6. https://doi.org/10.3354/meps09785

Klevjer, T.A., Martinez, Udane, Boyra, Guillermo, Røstad, Anders, Kaartvedt, Stein, Irigoien, Xabier, 2020. Integrated daytime EK60 echosounder data from Malaspina-2010 cruise. https://doi.org/10.1594/PANGAEA.923087

Kloser, R.J., Ryan, T., Sakov, P., Williams, A., Koslow, J.A., 2002. Species identification in deep water using multiple acoustic frequencies. Canadian Journal of Fisheries and Aquatic Sciences 59, 13.

Kloser, R.J., Ryan, T.E., Keith, G., Gershwin, L., 2016. Deep-scattering layer, gas-bladder density, and size estimates using a two-frequency acoustic and optical probe. ICES Journal of Marine Science 73, 2037–2048. https://doi.org/10.1093/icesjms/fsv257

Kloser, R.J., Ryan, T.E., Young, J.W., Lewis, M.E., 2009. Acoustic observations of micronekton fish on the scale of an ocean basin: potential and challenges. ICES Journal of Marine Science 66, 998–1006. https://doi.org/10.1093/icesjms/fsp077

Lavery, A.C., Wiebe, P.H., Stanton, T.K., Lawson, G.L., Benfield, M.C., Copley, N., 2007. Determining dominant scatterers of sound in mixed zooplankton populations. The Journal of the Acoustical Society of America 122, 3304–3326. https://doi.org/10.1121/1.2793613

Lawson, G.L., Wiebe, P.H., Ashjian, C.J., Gallager, S.M., Davis, C.S., Warren, J.D., 2004. Acoustically-inferred zooplankton distribution in relation to hydrography west of the Antarctic Peninsula. Deep Sea Research Part II: Topical Studies in Oceanography 51, 2041–2072. https://doi.org/10.1016/j.dsr2.2004.07.022

Lehodey, P., Conchon, A., Senina, I., Domokos, R., Calmettes, B., Jouanno, J., Hernandez, O., Kloser, R., 2015. Optimization of a micronekton model with acoustic data. ICES Journal of Marine Science 72, 1399–1412. https://doi.org/10.1093/icesjms/fsu233

Love, R.H., 1978. Resonant acoustic scattering by swimbladder-bearing fish. The Journal of the Acoustical Society of America 64, 571–580. https://doi.org/10.1121/1.382009

Lucca, B.M., Ressler, P.H., Harvey, H.R., Warren, J.D., 2021. Individual variability in sub-Arctic krill material properties, lipid composition, and other scattering model inputs affect acoustic estimates of their population. ICES Journal of Marine Science 78, 1470–1484. https://doi.org/10.1093/icesjms/fsab045

Lüdecke, D., 2018. ggeffects: Tidy Data Frames of Marginal Effects from Regression Models. Journal of Open Source Software 3, 772. https://doi.org/10.21105/joss.00772

Mackenzie, K.V., 1981. Nine-term equation for sound speed in the oceans. The Journal of the Acoustical Society of America, The Journal of the Acoustical Society of America 70, 807–812. https://doi.org/10.1121/1.386920

MacLennan, D.N., Fernandes, P.G., Dalen, J., 2002. A consistent approach to definitions and symbols in fisheries acoustics. ICES Journal of Marine Science 59, 365–369. https://doi.org/10.1006/jmsc.2001.1158

Mair, A.M., Fernandes, P.G., Lebourges-Dhaussy, A., Brierley, A.S., 2005. An investigation into the zooplankton composition of a prominent 38-kHz scattering layer in the North Sea. Journal of Plankton Research 27, 623–633. https://doi.org/10.1093/plankt/fbi035

Marohn, L., Schaber, M., Freese, M., Pohlmann, J.D., Wysujack, K., Czudaj, S., Blancke, T., Hanel, R., 2021. Distribution and diel vertical migration of mesopelagic fishes in the Southern Sargasso

Sea — observations through hydroacoustics and stratified catches. Mar. Biodivers. 51, 87. https://doi.org/10.1007/s12526-021-01216-6
Marouchos, A., Sherlock, M., Kloser, R., Ryan, T., Cordell, J., 2016. A profiling acoustic and optical system (pAOS) for pelagic studies; Prototype development and testing, in: OCEANS 2016 - Shanghai. Presented at the OCEANS 2016 - Shanghai, IEEE, Shanghai, China, pp. 1–6. https://doi.org/10.1109/OCEANSAP.2016.7485399
Mauchline, J., 1981. Measurement of body length of Euphausia superba Dana., in: BIOMASS Handbook. pp. 4–9.
Mazerolle, M., 2023. AICcmodavg: Model selection and multimodel inference based on (Q)AIC(c). R package version 2.3.2.
McClatchie, S., Thorne, R.E., Grimes, P., Hanchet, S., 2000. Ground truth and target identification for fisheries acoustics. Fisheries Research 47, 173–191.
McFadden, D., 1973. Conditional logit analysis of qualitative choice behavior.
McGehee, D.E., O'Driscoll, R.L., Traykovski, L.V.M., 1998. Effects of orientation on acoustic scattering from Antarctic krill at 120 kHz. Deep Sea Research Part II: Topical Studies in Oceanography 45, 1273–1294. https://doi.org/10.1016/S0967-0645(98)00036-8
Menkes, C., Allain, V., 2021. WARMALIS 1 cruise, Alis R/V. https://doi.org/10.17600/18000710
Olu, K., Allain, V., 2020. KANARECUP cruise, Alis R/V. https://doi.org/10.17600/18001103
Pakhomov, E., Yamamura, O., 2010. PICES Scientific Report No. 38 (No. 38). North Pacific Marine Science Organization (PICES).
Pearre, S., 2003. Eat and run? The hunger/satiation hypothesis in vertical migration: history, evidence and consequences. Biological Reviews of the Cambridge Philosophical Society 78, 1–79. https://doi.org/10.1017/S146479310200595X
Peña, M., Andrès, L., González-Quirós, R., 2023. Target strength of *Cyclothone* species with fat-filled swimbladers. Journal of Marine Systems 240, 103884. https://doi.org/10.1016/j.jmarsys.2023.103884
Peña, M., Cabrera-Gámez, J., Domínguez-Brito, A.C., 2020. Multi-frequency and light-avoiding characteristics of deep acoustic layers in the North Atlantic. Marine Environmental Research 154, 104842. https://doi.org/10.1016/j.marenvres.2019.104842
Peña, M., Villanueva, R., Escánez, A., Ariza, A., 2018. Opportunistic acoustic recordings of (potential) orangeback flying squid Sthenoteuthis pteropus in the Central Eastern Atlantic. Journal of Marine Systems 179, 31–37. https://doi.org/10.1016/j.jmarsys.2017.11.003
Perrot, Y., Brehmer, P., Habasque, J., Roudaut, G., Behagle, N., Sarré, A., Lebourges-Dhaussy, A., 2018. Matecho: An Open-Source Tool for Processing Fisheries Acoustics Data. Acoustics Australia 46, 241–248. https://doi.org/10.1007/s40857-018-0135-x
Proud, R., Cox, M.J., Brierley, A.S., 2017. Biogeography of the global ocean's mesopelagic zone. Current Biology 27, 113–119. https://doi.org/10.1016/j.cub.2016.11.003
Proud, R., Handegard, N.O., Kloser, R.J., Cox, M.J., Brierley, A.S., Demer, D., 2019. From siphonophores to deep scattering layers: uncertainty ranges for the estimation of global mesopelagic fish biomass. ICES Journal of Marine Science 76, 718–733. https://doi.org/10.1093/icesjms/fsy037
R Core Team, 2023. R: A Language and Environment for Statistical Computing. R Foundation for Statistical Computing.
Receveur, A., Menkes, C., Allain, V., Lebourges-Dhaussy, A., Nerini, D., Mangeas, M., Ménard, F., 2020a. Seasonal and spatial variability in the vertical distribution of pelagic forage fauna in the Southwest Pacific. Deep Sea Research Part II: Topical Studies in Oceanography 175, 104655. https://doi.org/10.1016/j.dsr2.2019.104655
Receveur, A., Vourey, E., Lebourges-Dhaussy, A., Menkes, C., Ménard, F., Allain, V., 2020b. Biogeography of micronekton assemblages in the natural park of the Coral Sea. Frontiers in Marine Science 7, 449. https://doi.org/10.3389/fmars.2020.00449
Sarmiento-Lezcano, A.N., Olivar, M.P., Caballero, M.J., Couret, M., Hernández-León, S., Castellón, A., Peña, M., 2023. Swimbladder properties of *Cyclothone* spp. in the northeast Atlantic Ocean

and the Western Mediterranean Sea. Frontiers in Marine Science 10, 1093982. https://doi.org/10.3389/fmars.2023.1093982

Scoulding, B., Chu, D., Ona, E., Fernandes, Paul.G., 2022. Erratum: ''Target strengths of two abundant mesopelagic fish species". The Journal of the Acoustical Society of America 151, 3398–3398. https://doi.org/10.1121/10.0011465

Scoulding, B., Chu, D., Ona, E., Fernandes, Paul.G., 2015. Target strengths of two abundant mesopelagic fish species. The Journal of the Acoustical Society of America 137, 989–1000. https://doi.org/10.1121/1.4906177

Scoulding, B., Gastauer, S., MacLennan, D.N., Fässler, S.M.M., Copland, P., Fernandes, P.G., Demer, D., 2017. Effects of variable mean target strength on estimates of abundance: the case of Atlantic mackerel (*Scomber scombrus*). ICES Journal of Marine Science 74, 822–831. https://doi.org/10.1093/icesjms/fsw212

Sobradillo, B., Boyra, G., Martinez, U., Carrera, P., Peña, M., Irigoien, X., 2019. Target Strength and swimbladder morphology of Mueller's pearlside (*Maurolicus muelleri*). Scientific Reports 9, 17311. https://doi.org/10.1038/s41598-019-53819-6

St. John, M.A., Borja, A., Chust, G., Heath, M., Grigorov, I., Mariani, P., Martin, A.P., Santos, R.S., 2016. A dark hole in our understanding of marine ecosystems and their services: perspectives from the mesopelagic community. Frontiers in Marine Science 3, 31. https://doi.org/10.3389/fmars.2016.00031

Stanton, T., Wiebe, P.H., Chu, D., Benfield, M.C., Scanlon, L., Martin, L., Eastwood, L.R., 1994. On acoustic estimates of zooplankton biomass. ICES Journal of Marine Science 51, 505–512. https://doi.org/10.1006/jmsc.1994.1051

Stanton, T.K., Chu, D., Wiebe, P.H., 1998. Sound scattering by several zooplankton groups. II. Scattering models. The Journal of the Acoustical Society of America 103, 236–253. https://doi.org/10.1121/1.421110

Stanton, T., Chu, D., 2000. Review and recommendations for the modelling of acoustic scattering by fluid-like elongated zooplankton: euphausiids and copepods. ICES Journal of Marine Science 57, 793–807. https://doi.org/10.1006/jmsc.1999.0517

Stanton, T.K., Sellers, C.J., Jech, J.M., 2012. Resonance classification of mixed assemblages of fish with swimbladders using a modified commercial broadband acoustic echosounder at 1–6 kHz. Can. J. Fish. Aquat. Sci. 69, 854–868. https://doi.org/10.1139/f2012-013

Trenkel, V.M., Berger, L., Bourguignon, S., Doray, M., Fablet, R., Massé, J., Mazauric, V., Poncelet, C., Quemener, G., Scalabrin, C., Villalobos, H., 2009. Overview of recent progress in fisheries acoustics made by Ifremer with examples from the Bay of Biscay. Aquatic Living Resources 22, 433–445. https://doi.org/10.1051/alr/2009027

Underwood, M.J., García-Seoane, E., Klevjer, T.A., Macaulay, G.J., Melle, W., 2020. An acoustic method to observe the distribution and behaviour of mesopelagic organisms in front of a trawl. Deep Sea Research Part II: Topical Studies in Oceanography 180, 104873. https://doi.org/10.1016/j.dsr2.2020.104873

Underwood, M.J., Utne Palm, A.C., Øvredal, J.T., Bjordal, Å., 2021. The response of mesopelagic organisms to artificial lights. Aquaculture and Fisheries 6, 519–529. https://doi.org/10.1016/j.aaf.2020.05.002

Verma, A., Kloser, R.J., Duncan, A.J., 2017. Potential use of broadband acoustic methods for micronekton classification. Acoustics Australia 45, 353–361. https://doi.org/10.1007/s40857-017-0105-8

Warren, J.D., Smith, J.N., 2007. Density and sound speed of two gelatinous zooplankton: Ctenophore (*Mnemiopsis leidyi*) and lion's mane jellyfish (*Cyanea capillata*). The Journal of the Acoustical Society of America 122, 574–580. https://doi.org/10.1121/1.2739433

Williams, K., Rooper, C.N., De Robertis, A., Levine, M., Towler, R., 2018. A method for computing volumetric fish density using stereo cameras. Journal of Experimental Marine Biology and Ecology 508, 21–26. https://doi.org/10.1016/j.jembe.2018.08.001

Yasuma, H., Sawada, K., Takao, Y., Miyashita, K., Aoki, I., 2010. Swimbladder condition and target strength of myctophid fish in the temperate zone of the Northwest Pacific. ICES Journal of Marine Science 67, 135–144. https://doi.org/10.1093/icesjms/fsp218

Ye, Z., 1997. Low-frequency acoustic scattering by gas-filled prolate spheroids in liquids. The Journal of the Acoustical Society of America 101, 1945–1952. https://doi.org/10.1121/1.418225

Young, J.W., Hunt, B.P.V., Cook, T.R., Llopiz, J.K., Hazen, E.L., Pethybridge, H.R., Ceccarelli, D., Lorrain, A., Olson, R.J., Allain, V., Menkes, C., Patterson, T., Nicol, S., Lehodey, P., Kloser, R.J., Arrizabalaga, H., Anela Choy, C., 2015. The trophodynamics of marine top predators: Current knowledge, recent advances and challenges. Deep Sea Research Part II: Topical Studies in Oceanography 113, 170–187. https://doi.org/10.1016/j.dsr2.2014.05.015

Highlights

- Acoustic-trawl surveys in scattering layers of West tropical Pacific.
- Forward scattering models applied to micronekton trawl sampling with a high species diversity.
- The difference of volume scattering between echosounder and modelled from trawl is variable within scattering layers.
- Reduced disparities between acoustic and trawl data in night mesopelagic layers and in trawls capturing a high density of fish with swimbladders.

Declaration of interests

☒ The authors declare that they have no known competing financial interests or personal relationships that could have appeared to influence the work reported in this paper.

☐ The authors declare the following financial interests/personal relationships which may be considered as potential competing interests: